Академия наук СССР

Academy of Sciences USSR

ИНСТИТУТ КОСМИЧЕСКИХ ИССЛЕДОВАНИЙ

SPACE RESEARCH INSTITUTE

T.K. Breus, K.I. Gringauz, M.I. Verigin

VENUS IONOSPHERE

(Proposals for VIRA - Venus International Reference Atmosphere)

Recommended for publication by N.S. Kardashev

117810 Москва, ГСП-7, Профсоюзная 84/32

Телетайп: 111325 ПАРСЕК

Москва

ACADEMY OF SCIENCES OF THE USSR

SPACE RESEARCH INSTITUTE

Пр-835

T.K. Breus, K.I. Gringauz, M.I. Verigin

VENUS IONOSPHERE

(Proposals for VIRA - Venus International Reference Atmosphere)

Recommended for publication by

N.S. Kardashev

1983

Content

I Sources of experimental data

Experimental data on the Venus ionosphere were acquired as a result of experiments performed on board the Soviet Venera-4,9,10 and the American Mariner-5,10 and Pioneer-Venus spacecrafts. According to the techniques used for their acquisition these data can be divided into two groups:

1. Distant observation data obtained by radiooccultations of the spacecrafts. The Mariner-5,10 radiooccultations were observed during their single pass near Venus Mariner Stanford Group, 1967; Kliore et al., 1967; Howard et al., 1974; Fjeldbo et al., 1975) whereas numerous radiooccultations of Venera-9,10 and Pioneer-Venus yielded the rich statistical material Aleksandrov et al., 1976 a, b; Jakovlev et al.,1976; Kliore et al., 1979 a,b .

2. Data of direct measurements in the Venus ionosphere density, temperature and composition of charged particles, were obtained by various plasma experiments made by means of retarding potential analyzers, electrostatic analyzers, mass spectrometers and Langmuir probes [Gringauz, Breus, 1969; Knudsen et al., 1979; Wolfe et al., 1979; Taylor et al., 1979a; Brace et al., 1979].

Since not only the wave ionizing solar radiation but also the solar wind and the electron fluxes precipitating into the ionosphere effect essentially on the Venus ionosphere formation, their measurements are of interest for the Venus ionosphere physics.

It should be noted that certain parameters of the ionosphere obtained by various techniques even from the same space probe differ significantly. The causes may be: methodical incertainities in determining ionospheric parameters from the results of satellite measurements in the actual atmosphere of Venus, different spatial resolutions of instruments, and different criteria used for identifying the structural features of any event. These causes have not been analyzed yet completely. Therefore, the Venus ionosphere more readily lends itself to an accurate qualitative rather than quantitative description in spite of many attempts made to do the latter. The other reason why the Venus ionosphere, in particular its nightside part, is impeded to be described quantitatively is the inherent non-stationary state of the Venus ionosphere. Hence, to describe qualitatively the Venus ionosphere it is necessary to make a larger scope of measurements with external conditions controled than that available at present.

Therefore, on constructing the model we put emphasis on the qualitative description of the Venus ionosphere features and of the processes occurring there.

Figures 1 and 2 present the electron density profiles n_e (h) in the Venus ionosphere over the dayside (Figure 1) and nightside (Figure 2) of the planet obtained during the Venera-9,10 radiooccultations [Aleksandrov et al., 1976a, b; Ivanov-Kholodny et al., 1979; Gavrik et al., 1980]. Of interest is the regular character of the dayside $n_e(h)$-profiles and their variability in the nightside ionosphere. Parallel with the main peak of the electron number-density, the lower peak of the ionization is also seen on many profiles. The latter peak is well resolved against the main one (or absent) in the nightside ionosphere and observed in the dayside ionosphere as a characteristic break on the $n_e(h)$ profile (Figures 1,2). The upper boundary of the ionosphere, the ionopause, manifests itself as a pronounced drop of the electron number-density (Figure 1).

Conventionally, the Venus ionosphere can be divided into three regions:

- the main and low peaks of the ionization;
- the ionopause;
- the intermediate region where the character of the electron number-density distribution is strongly dependent on the solar zenith angle.

II Main and lower peaks of ionization

Statistically reliable data on the main and lower peaks of the ionization in the Venus ionosphere were gathered in radiooccultation experiments.

The Pioneer-Venus orbit pericenter altitude was always $\gtrsim 150$ km and only in 8 cases in the night ionosphere this probe altitude was lower than ≈ 145 km [Colin, 1980]. This did not allow systematic measurements of the main peak region in situ.

a) Electron density in the ionization peaks

Figure 3 gives the information available about the electron number-density in the main, n_{em}, and lower, n_{el}, peaks of the ionization determined from the Veneras radiooccultation data. The information about n_{em} and n_{el} in the dayside ionosphere was taken from the papers [Cravens et al., 1981, Ivanov-Kholodny et al., 1979, Gavrik et al., 1980], the data about the nightside ionosphere - from [Kliore et al., 1979b; Aleksandrov et al., 1976b and Gringauz et al., 1979].

As is seen from Figure 3, n_{em} in the day ionosphere is gradually decreasing with increasing the zenith angle, SZA, from n_{e_o} = (5 to 7)x10^{-5} cm^{-3} for SZA = 0^o to 10^5 cm^{-3} for SZA = 90^o. The relative value of n_{em} - decrease is well described by the simple layer theory [Chapman, 1931]. This fact evidences that the main peak of the ionization, due to UV-radiation of the Sun is formed under the photochemical equilibrium conditions. The lower values of n_{e_o} = 5x10^5 cm^{-3} obtained from the Venera-9,10 radiooccultation data as compared with n_{e_o} = 7.4x10^5 cm^{-3} obtained from the Pioneer--Venus data are specified by the fact that the latter radiooccultation experiment was performed under the higher solar activity conditions ($F_{10.7}$ = (175 to 215)x$10^{-22}$$W \cdot m^{-2}$ Hz^{-1}) than the Venera-9,10 experiments ($F_{10.7}$ = (70 to 80)x$10^{-22}$$W \cdot m^{-2} \cdot Hz^{-1}$). The electron density dependence on the solar zenith angle in the lower peak of the ionization, $n_{e\ell}$, in the day ionosphere is also well described by Chapman's theory [1931]. This peak is also formed under the photochemical equilibrium conditions by the solar soft X-ray radiation but not the UV one.

In the Venus night ionosphere n_{em} and $n_{e\ell}$ are the 1.5 to 2 orders of magnitude less than in the day ionosphere. The electron number-density in both peaks over the night side of the planet is subjected to significant variations (Figure 3), in case of the lower peak $n_{e\ell}$ being frequently smaller than several hundreds of electrons in cm^3, the radiooccultation experiment sensitivity threshold.

b) Altitudes of the ionization peaks

Figure 4, plotted on the same experimental data as Figure 3, shows the solar zenith angle dependence of the height of the main h_m and lower h_1 peaks of the ionization in the Venus ionosphere. The heights of both peaks remain practically identical for SZA 70° at the dayside of the planet. But according to Chapman's theory [1931] in the case of the neutral atmosphere (independent of SZA) h_m and n_1 must be gradually increasing with growing SZA due to the fact that for larger SZAs the solar wave radiation must cover a greater path in the atmosphere to reach the same height. The constant character of h_m and h_1 is due to decreasing temperature in the upper atmosphere for larger SZAs that results in reducing the number-density of neutral particles and this in turn, compensates the radiation path length increase in the atmosphere [Gavrik et al., 1980; Cravons et al., 1981]. Both factors that affect the electron number-density peak height are not completely balanced, and the Pioneer-Venus data about h_m given in Fig. 4 illustrate the h_m decrease for SZA 70° followed by the h_m growth for SZA 82°.

Thus, the predominant effect of the neutral number-density decrease on the h_m height for SZA 70° changed into the growth of h_m for SZA = 82° predicted by Chapman's theory (Kliore, 1981).

In the night ionosphere for SZA 110° the average height h_m is practically constant, i.e. 143 km, but its pass to pass variations are significantly larger than those in the day ionosphere. The average height of the lower peak of the Venus ionosphere at night h_1 equals $\gtrsim$118 km [Kliore, 1981] and thus the distance between the main and lower peaks is $\gtrsim$ 25 km at this time that is approximately by two times higher than $(h_m - h_1)$ in the dayside ionosphere (see Figure 4).

III. Location and dynamics of the ionopause

The effect of the solar-wind dynamic pressure on the Venus ionosphere is a physical constraint on its day-side extent. The radio occultation profiles $n_e(h)$ the upper boundary of the ionosphere, i.e. the ionopause, manifests itself as an abrupt decrease of the electron density (see Fig. 1).

That the ionopause exists became known since the Mariner-5 radio occultation experiment (Mariner Stanford Grou 1967). Its systematic observations by Venera-9 and Venera--10 have led Ivanov-Kholodny et al. [1979] to the conclusio of a monotonically increasing dependence of the ionopause height, h_i, on the solar zenith angle (when SZA$\leq 80^o$), Figure 5. However, far more numerous direct measurements of the ionopause location made by the Pioneer-Venus probe have revealed its considerable variability, in addition to a general trend, height h_i increase with increasing SZA. Figure 5 (from [Elphic et al., 1980a]) shows, by crosses, the positions of the plasmapause, estimated from magnetic field measurements.

Variations of the dynamic pressure of the solar wind, is the reason why the ionopause height varies for the fixed SZA value. The dayside ionosphere, however, does not directly interact with the solar plasma. From the solar wind heated at the detached near-Venus shock front the ionosphere is separated by a region of stronger magnetic fields, i.e. by the magnetic barrier which serves as a 'membrane' that transferred the solar wind pressure to the ionosphere. The relationship between the dynamic pressure of the solar wind, the magnetic pressure in the magnetic barrier, the ionopause height and the pressure of ionospheric plasma under the ionopause was analyzed in several papers [Brace et al., 1980; Elphic et al., 1980a, b, Vaisberg et al., 1980] .

Figure 6 which is a combination of Figure 5b,c Brace et al., 1980 shows by solid circles the magnetic field pressure in the magnetic barrier over the ionopause as a function of the dynamic pressure of the solar wind and by circles - the ionopause height dependence on the magnetic field pressure. It is seen that the pressure in the magnetic barrier and the pressure due to the solar wind are approximately equal, the ionopause height is decreasing with increasing both pressures but depending on their value non-linearly. The ionospheric plasma pressure and the magnetic field pressure in the magnetic barrier are also approximately equal Alphic et al., 1980a,b . Even if dynamic pressures of the solar wind are high the day ionopause was not observed below 200 km (Figures 5,6).

Brace et al. [1979,b] pointed out the existence of the ionopause on the Venus night side too. In this ionospheric region the ionopause location is more variable than over the day and nightsides of the planet: sometime the night ionopause was observed at very low heights, 200 km, and sometime above 3500 km. Note that the Mariner-5 radiooccultation experiment observed the night ionosphere boundary at 3700km [Mariner Stanford Group, 1967]. Physical processes resulting in the ionopause presence over the planetary nightside have not been obvious yet and it is not clear whether this boundary is a quasi-stationary (as the day ionopause) or a dynamical formation.

IV. The ionosphere between the main ionization peak and the ionopause

The Pioneer-Venus systematic direct measurements are the basic source of information about the ionosphere between the main ionization peak and the ionopause. Only the upper limit of the ion number-density on the planetary night-side (Venera-4, [Gringauz, Breus, 1969]) and the data on the electron number-density(obtained by radiotechniques) were known before the Pioneer-Venus measurements were made (see Section II).

a) Diurnal variation of the ion composition

The Pioneer-Venus performed measurements of the ion composition using the radiofrequency ion mass spectrometer

(OIMS) [Taylor et al., 1979a,b; 1980]. The distribution and the temperature of the major ionospheric components could also be measured by means of a wide-angle retarding-potential analyzer [Knudsen et al., 1979a,b;1980b] . Figure 7 shows the diurnal variation of the densities of different ions obtained for 200 km: CO_2^+, O_2^+, NO^+, $CO^+ + N_2^+$, O^+, N^+, C^+, He^+ and H^+ plotted based on the OIMS data acquired during first two Venerian years of the probe operation. The data shown here were taken from the paper Taylor et al., 1980 but they were ordered in a decreasing sequence for ionic molecular weights.

The typical feature of the diurnal variation for the densities of heavy molecular ions in its abrupt fall at the terminator while passing to the night ionosphere; this fall is of 2 to 3 orders of magnitude (Figure 7). This fall is less expressed in case of light ions O^+, N^+, C^+; their density in the night upper ionosphere decreases by 1 to 2 orders of magnitude. The asymmetric bulge in the density of light ions H^+ and He^+ is observed at night, well-defined at dawn (Figure 7). The asymmetry in the diurnal distribution of H^+ is balanced by O^+ ion and molecular ions concentrating in the night upper ionosphere generally in the dusk so that the total density of ions has no a considerable dawn-dusk asymmetry [Taylor et al., 1980] .

The densities of all measured ions have the well-defined fluctuations in the night ionosphere and near the terminator (Figure 7) apparently connected with non-regular character of the solar wind and the interplanetary magnetic field geometry, that is why the night ionosphere behavior is unpredictable to a great extent [Taylor et al., 1980] .

b) Height distribution of the ion densities

Figures 8, 9 show the "height-profiles" of the density of various ions, $n_i(h)$, in the day and night ionosphere respectively, which are characteristic for the morphology of these regions to some extent [Taylor et al., 1980] . In the rigorous sense the given $n_i(h)$ dependences are not the height profiles since they were measured only along the Pioneer-Venus very flat trajectory near the pericenter and are distorted due to the effects of spatial inhomogeneities and time variations of different scales. May be, these effects cause the O_2^+-density maximum seen in Figure 8 (this ion is predominant in the main peak of the ionospheric ionization) and observed at 175 km whereas the ionization peak has never been observed at such heights in the day time according to radio-occultation data (see Figure 4 taken from the paper of Gravens et al. 1981). Of interest is also the O^+-density value in the main peak of the night ionosphere ionization determined from the mass spectrometer data as equal to about 1.5x $\times 10^{+5}$ cm^{-3}. In this regions the values of n_{em} (most frequently observed in radiooccultation experiments) are approximately by 5 times lower, (see Figure 3). Such a discrepancy is not the only among the scope of experimental data obtained via the Pioneer-Venus instruments. For example, the neutral atmosphere model (which is significant for ionosphere physics) constructed upon the neutral particle mass-spectrometer (ONMS) data used the 1.63-fold increase in the density values Hedin et al., 1983 . It is evident that it is necessary to treat very carefully the quantitative conclusions made upon the measurements in the Venus vicinity, and to analyze thoroughly the discrepancies in the data of various experiments, as it has been mentioned in Section I.

The qualitative analysis of mass-spectrometric observations shows the prevalence of O_2^+-ion in the lower ionosphere. When the height is increasing O^+ion becomes predominant. It is essential that the night ionosphere consists of the same ions as the day one (cf. Figures 8,9). The irregularity mentioned above manifests itself for the most part of measurements in the night ionosphere; its example is the buldge in n_i observed 230 km (see Figure 9) Taylor et al., 1980

c) <u>Thermal structure of the ionosphere</u>.

Electron temperature in the Venus ionosphere can be measured directly only by means of two instruments: a Langmuir probe (OETP) [Brace et al., 1979, 1980; Theis et al., 1980 and a retarding potential analyzer (ORPA) Knudsen et al., 1979a,b; Miller et al., 1980], temperature of the dominant ions can be measured only by means of ORPA. Figure 10 combines the height profiles of ions, T_i, and electrons, T_e, for different solar zenith angles taken from the paper [Miller et al. 1980] .

The feature of the electron temperature distribution is the very high values and the weak dependence on a zenith angle. Superthermal photoelectrons and the solar wind energy transferred through the ionopause might be the sources which maintain the high temperature of electrons. The first source, however, cannot maintain the high values of Te during the whole night, and evidently the heat flows through the ionopause contribute much to Te. Knudsen et al. 1980a and Hoegy et al. [1980] made such a conclusion based on measurements of the fluxes of superthermal photoelectrons in the day ionosphere and on an analysis of the equations for heat conduction. Before this, Knudsen et al. [1979b] believed that only photoelectrons can maintain the observed values of Te.

Above ~300 km the ion temperature as well as Te does not depend on a solar zenith angle (Figure 10) except for the range $150^\circ \lesssim$ SZA $\lesssim 180^\circ$ where Ti increases approximately by two time reaching 5000°K, and according to Miller et al. [1980] exceeds Te. Miller et al. [1980] suggest a speculative explanation for the increase of T_i and assumed that this growth is caused by transforming the energy of the directional motion of the supersonic fluxes of ions into the heat energy as a result of convergence on the antisolar axis of the ion fluxes transported from the day side.

The rise of T_i with the increase of SZA within the height range $\lesssim$ 300 km after the terminator (FIG. 10) is obviously associated with the decrease in this region of the ion cooling rate by neutrals due to the neutral atmosphere density fall behind the terminator [Miller et al., 1980].

d) <u>Plasma transport from the day-side ionosphere</u>

The data of two experiments: OIMS [Taylor et al., 1980] and ORPA [Knudsen et al., 1980b] indicate the presence of the plasma horizontal transport in the Venus ionosphere. According to these data the plasma convective transport velocities $\vec{V}_c$ can be considerably high: from $\lesssim 1$ km/sec at the heights $\lesssim 200$ km to several kilometers per second at higher heights. The following factors obviously cause the plasma transport from the day ionosphere at different heights:

- the viscous-like interaction with the solar wind in the ionopause vicinity [Perez de Tejada, 1980] ;
- the ion density gradient near the terminator [Knudsen et al., 1981]; and
- the winds in the neutral atmosphere involving ions at lower heights.

At present it is difficult to judge about the reliable determination of the plasma transport velocity $\vec{V}_c$ from the data of both experiments because the method for such determinations and the primary experimental data used have not been published yet in principle. It is not clear whether the satellite potential was taken into account in determining V_c from the OIMS data. Knudsen et al. [1980, b] state that this value was known with an accuracy of ± 0.1V that seems to be rather optimistic. Besides the satellite potential was determined in the other mode of ORPA operation, not simultaneously with measurements of the ion retardation curves. These curves were measured for every $\vec{V}_c$ at three points of the satellite trajectory spaced by ~200 km. For the fastly and unpredictably changing night ionosphere such measurements become in certain [Taylor et al., 1982].

Nevertheless, the fact itself of the convective motions of the plasma in the ionosphere and the orders of the velocity values observed sometimes there raise no doubts.

The plasma convection velocities and the ionopause heights in the vicinity of the terminator are usually used for estimating the flux of O^+ ions transported to the night ionosphere of Venus. The estimates of the transported flux of ions are then used for calculating the diffusive flux of O^+ ions downward over the night side of Venus [Taylor et al., 1980; Knudsen et al., 1980b]. However, the further destiny of ions transported from the day side of the planet is not known, and the assumption that the significant part of convecting ions should diffuse downward over the whole night side of the planet, seems to be some oversimplification of the problem.

V. Non-stationary and small-scale events in the Venus ionosphere

Above we discussed mainly the large-scale events characterizing the ionosphere as a whole. However, direct measurements in the ionosphere revealed certain interesting small-scale events. Some of them affect undoubtedly the global features of the ionosphere. To describe them briefly it is convenient to use the scheme of the processes occurring in the Venus vicinity developed by Brace et al. [1983] (Figure 11).

The wave-type irregularities of the ionospheric plasma which were interpreted by Brace et al. [1980, 1982a] as surface waves on the ionopause were often observed in the vicinity of the day-side ionopause. The so-called clouds of the ionosphere-type plasma observed above the ionopause can be also associated with these waves [Knudsen et al., 1979a; Brace et al., 1980]. As a rule, these plasma clouds are observed downstream of the wave-type structures (Figure 11), and obviously are the next stage of the processes of the losses of ionospheric plasma due to its interaction with the solar wind [Brace et al., 1982,a]. The magnetic field envelopes the plasma clouds and contributes to their acceleration [Russell et al., 1982].

Flux ropes observed in the day ionosphere of Venus can be the other result of these wave processes in the vicinity of the magnetopause [Russell and Elphic, 1979]. The characteristic scale of these structures in the lower ionosphere is 10 to 20 km increasing slightly at higher heights where while recording the magnetic fields twisted into flux ropes the plasma density decrease is also observed. Any regular magnetic field has not been found in 70% of observations in the Venus ionosphere [Luhmann et al., 1980].

One more structure - the magnetic belt - was sometime observed in the day ionosphere of Venus and was connected with measurements of the magnetic field [Russell et al., 1983]. The magnetic belt is the horizontal large-scale steady-state magnetic field with a strength frequently higher than 100 γ that sometime can be observed in the lower ionosphere for SZA $\leq 50^{\circ}$ [Zuhmann et al., 1980]. The appearance of these large-scale fields correlates with the periods of high dynamical pressures in the solar wind. In contrast to Cloutier et al. [1981] the magnetic experiment authors believe that the magnetic belt is not a steady-state structure but the remaider (slowly decaying at low heights) of the intense magnetic fields which have been formed there when the dynamic pressure in the solar wind was extremely high, and remained alive for some time after its decrease [Russell et al., 1983]. Thus, we can suggest that over the day side of Venus two layers of the strong magnetic field exist simultaneously for some time - in the magnetic barrier and in the magnetic belt. However, many events associated with the observations of the intense magnetic fields in the ionosphere can be evidently explained traditionally. We can assume that they are the result of the non-monotonous charge in a distance between the magnetic barrier and a satellite during its motion through the ionosphere. Such a non-monotonous change in the satellite position relative to the ionopause can be caused, for example, variations of the dynamic pressure in the solar wind, the specific shape of the ionopause for high dynamical pressures, large-scale wave changes in its shape under these conditions and so on.

In the night ionosphere the non-stationary events are better pronounced than in the day ionosphere. The first measurements in the night ionosphere revealed that sometime it disappear completely up to a height of ~170 km [Taylor et al., 1979b]. At this time the ion number-density in the night upper ionosphere is by 3-4 orders of magnitude less than in the case of the established night ionosphere. However, the radiooccultation data(but obtained at the different latitude) showed that in the case of the depleted ionosphere the plasma density changes inconsiderably in the vicinity of the ionization peak. For example, in case of observations of the depleted ionosphere Taylor et al., 1979b in the vicinity of the main and lower peaks of the ionization the electron number-density was $n_{em} = 10^4$ cm^{-3}, $n_{el} = 7 \cdot 10^3$ cm^{-3}, respectively, i.e., close to the usual data obtained for this region (see Figure 3) [Taylor et al., 1982]. The observed "independence" of the plasma density variations in the upper and lower ionosphere can apparently indicate that their formation is provided for different sources of the ionization and occurs under different physical conditions: in the upper night ionosphere the dynamical processes of the plasma transport from the day side of the planet are essential, but in the vicinity of h_m it is the collision ionization by precipitating electrons (see also Section V(b)).

During several passages of Pioneer-Venus in the night ionosphere its spatial inhomogeneity was detected which is associated with the presence in this region of the horizontal plasma layers and the troughs in the plasma density, the so-called holes [Brace et al., 1980]. The satellite measurements of the plasma density revealed the peculiarities symmetric relative to the periapsis (i.e., located at the same heights) that are the indication of the horizontal stratification of the night ionosphere. These horizontal layers are very extended since they can be observed at the inbound and outbound trajectories of the satellite at the distances of several thousand of kilometers from these regions. The extent of these horizontal layers indicates that the formation of the global stratification of the night ionosphere is connected with the global processes [Brace et al., 1980].

Holes in the night ionosphere are obviously the most stable structures [Brace et al., 1982b] (Figure 11). They are the pair large-scale formations with a characteristic size of ~1000 km piercing the ionosphere down to the lowest heights, and possess the practically vertical magnetic field more intense as compared with that of adjacent regions [Brace et al., 1982b, Luhmann et al., 1981]. The plasma density in the "northern" and "southern" holes (they compose a pair) falls by two orders of magnitude in comparison with the ionosphere surrounding them. The electron temperature is $\sim 2000^{\circ}$ that is substantially lower than in the ionosphere except the portion of a hole with the minimum n_e values where T_e reaches $\sim 20{,}000^{\circ}$. Holes are assumed to be formed due to the electric fields parallel to almost the radial magnetic field in the ionosphere [Grebowsky and Curtis, 1981]. They are apparently the regions of the intense escape of ionospheric plasma and the regions where accelerated electrons penetrating from the magnetic tail heat electron gas up to high temperatures [Nagy et al., 1983].

VI. Modeling the ionospheric processes

The first electron density profiles measured in the Venus ionosphere gave rise to modeling physical processes occurring there [Mariner Stanford Group, 1967; Kliore et al., 1967]. At the initial modeling stage one believed that CO_2^+ [McElroy, 1969; Whitten, 1970; Herman et al., 1971] is the dominant ion in the main ionization peak. However, it became clear then (even before the Mariner-10 radiooccultation experiment Howard et al., 1971) that O_2^+-ion dominates in the main ionization peak [Kumar, Hunten, 1974] . The ionospheric model developed by Nagy et al. [1975] described the most features of $n_e(h)$-profiles observed in both above experiments. The results of the Venus ionosphere modeling initiated by the Mariner-5,10 and Venera-9,10 radiooccultation experiments are rather completely reviewed in the papers by Whitten, Colin [1974] and Shunk, Nagy [1980] . We will describe the current state of the Venus ionosphere modeling problem, i.e., after the Pioneer-Venus direct measurements.

All the theoretical models of the Venus ionosphere published until recently are one-dimensional except calculations made by Whitten et al. [1982] and Cravens et al. [1983] who tried to include the effect of horizontal gradients of ionospheric parameters on the ionization height profiles. The results of modeling the day and night ionospheres can be discussed separately as the ionosphere models are one-dimensional.

a) <u>Modeling the day ionosphere composition</u>

General processes in the dayside ionosphere were defined as a result of in situ measurements of the Venus atmosphere and ionosphere composition [Bauer et al., 1979] . The solar UV-radiation is the dominant source of ions on the dayside. Ions formed due to photoionization (and due to secondary ionization by photoelectrons) take part in some ion-molecular reactions and finally recombine with electrons. The generally accepted scheme of chemical processes in the Venus ionosphere is given in Figure 12 [Nagy et al., 1983].

To estimate the electron density n_{em} in the vicinity of the main ionization peak, h_{max}, there is no necessity to include all these processes. In the vicinity of h_{max} O_2^+ is the dominant ion (see Figures 8, 13). Though the ion production rate is the maximum in this region for CO_2^+-ion, CO_2^+-ions are effectively transformed into O_2^+-ions as a result of the following ion-molecule reactions:

$$CO_2^+ + O \rightarrow O_2^+ + CO, \quad k = 1.6\times10^{-11}\ cm^3\ s^{-1}$$

$$CO_2^+ + O \rightarrow O + CO_2, \quad k = 9.6\times10^{-11}\ cm^3\ s^{-1}$$

$$O^+ + CO_2 \rightarrow O_2^+ + CO, \quad k = 9.4\times10^{-10}\ cm^3 \cdot s^{-1}$$

Then, most of O_2^+ ions recombine with electrons:

$$O_2^+ + e \rightarrow O + O, \quad \alpha = 1.6\times10^{-7}\left(\frac{800}{T_e}\right)^{0.55}\ cm^3\ s^{-1}$$

Under the photochemical equilibrium conditions this simplified scheme provides the sufficiently exact equation for n_{em} Gravens et al., 1981 :

$$n_{em} \approx 520\sqrt{P}\cdot T_e^{0.275} \qquad (1)$$

where P is the ion production rate in $cm^{-3}\cdot s^{-1}$, and T_e is the electron temperature in ^oK.

However, to calculate the densities for other ions measured in the Pioneer-Venus direct experiments [Taylor et al., 1979a, 1980] one must consider several tens of ion-molecule reactions [Izakov et al., 1981; Nagy et al., 1980]. The calculations made by Izakov et al. [1981] based on Niemann et al.'s [1980] model at the neutral atmosphere including 45 ion-molecule reactions confirm their reasonable agreement with experimental data (Figure 8). A bend on the calculated O_2^+-profile below the main ionization peak (Figure 8) is a result of forming in this height region the lower peak due to the solar soft X-ray radiation. A similar bend can be observed on the radiooccultation $n_e(h)$-profiles of the dayside ionosphere.

Above 180 to 200 km the photochemical equilibrium conditions are violated in the day ionosphere. The non-local processes of diffusion become significant due to increase of the free path lengths for ions, and hence height profiles for different ions are usually calculated in a diffusion approximation [Bauer et al., 1979; Nagy et al., 1979, 1980; Gavrik et al., 1982]. In this case the one-dimensional simplified equations of continuity and momentum are solved together [Nagy et al., 1980]:

$$\frac{\partial F_s}{\partial h} = P_s - L_s ; \qquad (2)$$

$$F_s = -D_s n_s \left[\frac{1}{n_s} \frac{\partial n_s}{\partial h} + \frac{n_s g}{kT_s} + \frac{T_e/T_i}{n_e} \frac{\partial n_e}{\partial h} + \right. \qquad (3)$$

$$\left. + \frac{1}{T_i} \frac{\partial}{\partial h} (T_e + T_i) + \alpha_s / T_i \frac{\partial T_i}{\partial h} \right]$$

where F_s is the vertical diffusive flux of ions of S-type; D_s and α_s are the coefficients of diffusion and thermal diffusion, respectively; g is the free fall acceleration; P_s and L_s are the rates of ion production and losses, respectively. Figure 13 (dotted lines) illustrates the calculation results for SZA = 0^o obtained by Nagy et al. [1980] with this approximation for ions O_2^+, O^+, CO_2^+, C^+, N^+, He^+ and H^+ and with the approximation of photochemical equilibrium for ions N_2^+, NO^+ and CO^+. The solid lines in Figures 13 and 8 show the number densities of ions mentioned above determined from mass spectrometer data [Taylor et al., 1980] acquired on the 186th orbit of Pioneer-Venus (these measurements were started at SZA = 11^o). The comparison of the estimated $n_i(h)$-profiles and the experimental data indicates that in general we understand now the character of physical and chemical processes that control a height distribution of ions in the day ionosphere of Venus below the ionopause though many significant details need their further refine [Nagy et al., 1980].

Notice, however, that increasing the density values used in the neutral atmosphere model [Hedin et al., 1983] by a factor of 1.63 (see Section IV) we can obtain better agreement between the calculated and experimental data (estimates obtained by [Izakov et al. 1981] and [Nagy et al. 1980]).

The model calculations described above, evidnetly, can not be used near the ionopause and the terminator where the effects of the convective transport of plasma neglected in Eqs (2), (3)) become essential. If only the possible horizontal transport of the plasma is taken into account we can write instead of (2):

$$u_x \frac{\partial n_s}{\partial x} + n_s \frac{\partial u_x}{\partial x} + \frac{n_s u_x}{R} \, cth\left(\frac{x}{R}\right) + \frac{\partial F_s}{\partial h} = P_s - L_s \qquad (4)$$

where x is the arc length counted from the subsolar point; R is the radial distance from the planet center. If u_x and $\frac{\partial u_x}{\partial x}$ values are assigned from any considerations, the equation (4) can be easily solved. The results by Cravens et al.'s paper [1983] referred to the day ionosphere provide that for $u_x \sim$ 1 km/s independent of X and h the effect of the horizontal velocity to the height profiles of ions is insignificant When the velocities are high and can be specified by the expression

$$u_x(x, h) = \sin\left(\frac{x}{R}\right)\left[1 + 0.012(h-200)\right] \text{km}\cdot\text{s}^{-1} \qquad (5)$$

i.e., linearly increasing from 1 km/s at h = 200 km to 5 km/s at h = 533 km, the ion densities are obtained somewhat less than those in the model proposed by Nady et al. [1980] due to plasma escape from the day ionosphere. The difference in the ion number-densities for the both models can reach in this case 20-80% for individual ions. The fact that Cravens et al. [1983] in their model describe the horizontal plasma velocity by external factors (assignment of u_x is equivalent to the introduction of additional sources/drains of plasma) does not permit this model to be considered as two-dimensional one in a strict sense.

The model of Whitten et al. 1982 is also quasi-two dimensional which can be applied to a narrow region near the terminator: $80^{\circ} \lesssim SZA \lesssim 100^{\circ}$. Using the simplified equation (4) Whitten et al. [1982] calculated the horizontal velocities of plasma in the vicinity of the terminator which are initiated by a plasma pressure gradient in this region. The obtained values of u_x correspond to the experimental ones but the model is rather qualitative than quantitative due to many simplifying assumptions.

b) <u>Ionization sources in the night ionosphere</u>.

Until 1967 the ionosphere was considered to be practically absent over the night side of Venus. Such a conclusion was made basing on the fact that during the very long Venesian night ($\sim$58 earth days) all ions transported from the dayside, must recombine even if their transport velocity was equal to that of a four-day superrotation of the upper atmosphere. The Mariner-5 radiooccultation experiment results showed the fallibility of these conclusions and encourage the attempts to explain the existence and to model the distribution of the plasma in the night ionosphere of Venus. The solar wind plasma turbulized behind the planetary bow shock front partly penetrating into the Venus atmosphere, cosmic rays, the scattered solar electromagnetic radiation, He^+-ions transported from the dayside and metal ions, meteorite ionization and so on were considered as possible sources of the night ionization : [-Mariner Stanford Group, 1967; Gringauz et al., 1968; Butler and Chamberlain, 1976; McElroy and Strobel, 1969] . All these sources of ionization neither explained satisfactorily the observed n_e -values nor use direct experimental data.

Until recently all model calculations of the night ionosphere have been performed practically identically to the procedure adopted for the day ionosphere, i.e., including only chemical processes and diffusion. Such an approximation is not obviously valid for the regions above several tens of kilometers over the main ionization peak, h_m, where the non-stationary processes and the convective transport of plasma become essential. To describe globally the supersonic plasma flow in the upper night ionosphere, the other equations are necessary. A study of the kind was not performed and good grounds hardly exist for making any physical conclusions based on a comparison of the variable (especially in this region) results of plasma experiments with the calculations carried out in a diffusion approximation.

In the vicinity of h_m model calculations of the night ionosphere become more valid from the physical viewpoint. The ionization source nature differs them from the similar calculations in the day ionosphere. However, in this region a quantitative comparison of the model and experimental data carries a few information content since almost always the agreement between experimental data about the night ionosphere (alternating widely) and the Venus atmosphere (see Sections 2 to 5) can be reached by choosing parameters of the ionization sources being variable too.

It is prematurely now to speak about the availability of the model that describes reliably physical processes in the night ionosphere of Venus. We will pay below our attention generally to the role of various ionization sources in different regions of the night ionosphere. Together with the results of measurements in the night ionosphere we will use only qualitative rather than quantitative results of the model calculations.

The first effective source of the night ionosphere ionization was detected during the Venera-9, 10 measurements of the fluxes of electrons with the energies of several tens of electronvolts in the optical shadow of the planets [Gringauz et al., 1976a, b]. Gringauz et al. [1976c, 1977a] calculated the electron impact ionization of the Venus atmosphere and revealed the correlation between n_{em} and the fluxes j_e of ionizing electrons. This resulted in the conclusion [Gringauz et al., 1977b, 1979] that the fluxes of electrons with energy of several tens of electronvolts detected by Venera-9, 10 are responsible for forming the main ionization peak in the night ionosphere.

Points on Figure 14 show all measured values (from Venera-9,10) of the integral electron fluxes j_e in the optical shadow of Venus with four values of a retarding voltage: 20, 40, 80 and 150V by means of a wide-angle retarding potential analyzer [Gringauz et al., 1983]. As seen from the Figure the scatter of j_e values during measurements was 2 orders of magnitude. This scatter qualitatively corresponds to that of n_e measurements which was approximately one order of magnitude (Figure 3) since $n_{em} \sim \sqrt{j_e}$.

The thin broken line in Figure 14 gives the energy spectrum of electrons measured on October 28, 1975 from Venera-9 for SZA=142°. The estimated n_e(h)-profile formed due to the effect of such electrons on the Venus atmosphere (the data about the night atmosphere were taken from the paper of Nieman et al. 1979) is shown in Figure 2 by a dotted line [Gringauz et al., 1981]. The similarity of the estimated and experimental profiles is obvious (the experimental profile was measured 11 minutes later on the same day for SZA=150°.

Pioneer-Venus measured the similar (to Venera-9, 10 ones) fluxes of electrons with the energy of several tens of electronvolts in the Venus ionosphere in situ by means of two independent instruments [Intriligator et al., 1979; Spenner et al., 1981]. The solid line in Figure 14 presents a typical electron spectrum in the night ionosphere (H = 244 km, SZA = = 125) plotted upon ORPA data [Spenner et al., 1981]. For convenience in a comparison the data of both experiments are presented as the electron downward fluxes per 1 cm^2 instead of omnidirectional fluxes (by 4 times more intense) as it has been done in the Gringauz et al.'s paper [1983]. The height dependence of the electron fluxes and their considrable anisotropy were not revealed [Spenner et al., 1981].

Thus, it is established reliably that the electron fluxes precipitating into the night ionosphere are a source of its ionization which can form $n_e(h)$-profile similar to that observed in radiooccultation experiments in the vicinity of h_m. Also note that the vertical intensity of the atomic oxygen glow (1304Å) estimated in the model of Gravens et al. [1983] is equal to 10R. This intensity is determined by electrons precipitating into the night ionosphere and agrees with the typical intensities of the glow obtained from the Pioneer-Venus UV-spectrometer data [Stewart, 1982].

The other source which maintains the night ionosphere of Venus was suggested after the Pioneer-Venus mass-spectrometric measurements [Nieman et al., 1979]. Such a source can be O^+ ions transported from the day side of the planet at heights 200 km. Diffusing downward O^+ ions take part in ion-molecular reaction with CO_2 forming O_2^+-ions predominant in the main ionization peak. Spenner et al. [1981] believe that O^+ transport is the dominant source of forming the main ionization maximum in the night ionosphere. The model calculations of the night ionosphere considering this source of the ionization are based, however, on the indefinite estimates of the O^+ ion fluxes through the terminator. The further behavior of these ions and the value of their downward diffusion flux into the dense layers of the night atmosphere, was not determined in the experiment. Systematic errors in the paper of Spenner et al. [1981] were analyzed in detail by Gringauz et al. [1983].

It has been noted in Section V that in the case of observations of the "depleted" upper ionosphere of Venus the plasma density in this region turned out to be by 3-4 orders less than in the established case. Apparently, within the same or even within the wider limits the diffusive downward flux of O^+ ions can vary. Hence, this ionization source becomes "too much variable" to determine the density n_e in the vicinity of $_{max}$ where its characteristic variations amount to only one order of magnitude.

When in the vicinity of h_m the only ionization source dominates, the height profiles of different ions have the following qualitative features. If O^+ ions diffusing downward are the only source of O_2^+-ions, their height profiles must be rigidly "interconnected", in this case the maximum of O_2^+-density must be observed on the background of abrupt fall of O^+ density. Since the height scale of carbon dioxide, $H_{CO_2} = 3$ km, is characteristic for O^+ losses in O_2^+ production, the maxima of the height profiles for both ions can be located at a distance of an order of several height scales for CO_2 [Gringauz, et al., 1983]. It is also obvious that the main ionization peak is formed in this case under the diffusive rather than chemical equilibrium (F_2-layer) conditions.

If the fluxes of ionizing electrons are responsible for forming the main maximum of O_2^+, the chemical equilibrium conditions (F_1-layer) are met in the vicinity of h_m resulting in infinit growth of O^+-density with increasing the height h. However, when h_m is increasing the diffusion processes become predominant and the O^+maximum is formed under the diffusive equilibrium conditions. In such a case the O^+-to-O_2^+ maxima distance is not determined by the height scale for CO_2 and can be greater than in the first case.

Taylor et al. [1982] published the results of detailed mass-spectrometric measurements of the ion composition in the vicinity of the night ionosphere obtained during the Pioneer-Venus two passes across this region. Figure 15a presents the smooth curves plotted over experimental points taken from Figure 5 of the above paper. As is seen, the distance between the maxima of the number-densities for O_2^+- and O^+-ions was 15 km, i.e., 5 H_{CO_2}. Approximately the same distance was between these maxima in the other example considered by Taylor et al. [1982] (see also Figure 9). Such distances are apparently an argument in favour of a conclusion that the main ionization maximum is formed due to precipitating electrons.

The other qualitative feature of the height profiles of ions shown in Figure 15a is the increase of the scale height for O_2^+ and O^+ ions at 170-180 km, i.e., in the vicinity of O^+-maximum. Such a change in the scale height for O_2^+ and NO^+ ions indicates evidently the passage from the chemical to diffusive equilibrium in the vicinity of O^+-maximum. In this case the O_2^+-maximum. In this case the O_2^+ ionization maximum is under the chemical equilibrium conditions. This fact (as it has been mentioned above) can be a qualitative argument in favour of the predominant role of a mechanism of the impact ionization by electrons in the vicinity of h_m.

With the height increasing over h_m, the non-stationary processes start to be more substantial as well as the convective transfer of plasma. Then the contribution of O^+ ions transported from the dayside of the planet to the ionic ionosphere formation gets more essential (see Section V). The both ionization sources discussed above refer to the upper maximum. To explain the low maximum it is necessary one should consider the other sources, for example: the fluxes of energetic ions from the plasma layer [Gringauz et al., 1981], the fluxes of more energetic electrons [Kliore et al., 1979b] and so on.

To explain the very high number-densities of O_2^+ ($10^5 cm^{-3}$) and O^+ (10^4 cm^{-3}) in the vicinity of h_{max} obtained from the OIMS mass-spectrometric measurements (Figure 15a), Taylor et al. 1982 assumed the existence of certain additional ionization mechanisms in the night ionosphere. However, the authors of this paper compared the mass-spectrometric results (the broken line in Figure 15b) with the radiooccultation results (crosses in Figure 15b) and made a conclusion about their reasonable agreement. Indeed, as seen from Figure 15b, the mass-spectrometric and radiooccultation data differ from each other by 3-4 times (see the dotted line of the total number-density n_e plotted from Taylor et al.'s data 1982). It is evident that first of all the cause of such discrepancies must be cleared up, and before this one should be very careful with quantitative results in developing physical models (it has been already noted in Section IV).

c) Modeling the thermal structure of the ionosphere

Modeling calculations of the thermal structure are based on the equation for heat conduction of the electron and ion gas:

$$\frac{3}{2} n_{e,i} K \frac{\partial T_{e,i}}{\partial h} - \frac{\partial}{\partial h}\left(K_{e,i} \frac{\partial T_{e,i}}{\partial h}\right) = Q_{e,i} - L_{e,i} \qquad (6)$$

where $K_{e,i}$ are the thermal conductivity; $Q_{e,i}$ and $L_{e,i}$ are the heating and cooling rates, respectively. Besides of heating by the solar EUV radiation the energy inflow must be taken into account that is due to the interaction with the solar wind in the ionopause vicinity.

Photoelectrons formed by ionization of the atmospheric neutral components loss their energy as a result of elastic and inelastic collisions with neutrals and of Coulomb collisions with thermal electrons. The energy obtained by thermal electrons from photoelectrons and due to superelastic collisions with neutrals determines the excess of Te over T_i and T_n. It is transfered to ions via Coulomb collisions and to the neutral components of the atmosphere via elastic and inelastic collisions. Exothermic chemical reactions and Joule heating are the additional sources of thermal energy of ions.

The model calculations base on the solution of (6) are in reasonable agreement with the measurements of day temperature of electrons and ions [Knudsen et al., 1979a,b; Brace et al., 1979a; Cravens et al., 1979, 1980] if there exists the additional (not connected with EUV) inflow of heat, and/or transfer coefficients are modified in (6). There are grounds for such changes.

The Pioneer-Venus experiment for measuring the electric fields revealed the presence of whistler-type waves in the transient region which are attenuating fastly on the ionopause [Scarf et al., 1979] . It is unknown what part of their energy is reflected from the ionopause but the upper energy limit ($3x10^{10}$e cm^{-2} s^{-1}) is by two orders of magnitude higher than the energy flux necessary for sustaining high values of T_e in the day ionosphere.

Figure 16 presents the results of calculations made by Nagy et al. [1980] of the profiles T_e, T_i and T_n in the day ionosphere for SZA = 60^o. These calculations took into account the changes in the thermal condictivity of electron gas due to the magnetic field fluctuations; the energy inflow to ions and electrons through the ionopause which is not connected with EUV radiation, was equal to $5x10^9 eV \cdot cm^{-2} \cdot s^{-1}$ and $3x10^7 eV \cdot cm^{-2} \cdot s^{-1}$, respectively. Regardless of the agreement between the experimental and estimated profiles of temperature the role of each above-discussed process in forming the thermal structure of the day ionosphere was not established unambiguously due to a great number of free parameters used in calculations [Nagy et al., 1983].

Energetics of the day ionosphere is more understandable than that of the nightside. In this region the heating by EUV radiation and whistlers is absent but precipitating electrons and the supersonic fluxes of ions contribute to the thermal balance.

References

Aleksandrov,Yu.N., M.B.Vasil'ev, A.S.Vyshlof, V.M.Dubrovin, A.L.Zaitsev, M.A.Kolosov, A.A.Krymov, G.I.Makovoz, G.M.Petrov, N.A.Savich, V.Z.Samovol, L.N.Samoznaev, A.I.Sidorenko, A.F.Khasyanov, D.Ya.Shtern, Preliminary results of two-frequency radioscopy of the daytime ionosphere of venus from Venera 9 and Venera 10, Kosmich. Issled., 14, 819-823, 1976 a.

Alexsandrov,Yu.N., M.B.Vasil'ev, A.S.Vyshlof, G.G.Dolbezhev, V.M.Dubrovin,A.L.Zaitsev, M.A.Kolosov, G.M.Petrov, N.A.Savich, V.Z.Samovol, L.N.Samoznaev, A.I.Sidorenko, A.F.Khasyanov, D.A.Shtern, Nighttime ionosphere of Venus from the results of two-frequency radioscopy from Venera 9 and Venera 10, Kosmich. Issled., 14, 824-827, 1976 b.

Bauer,S.I., T.M.Donahue, R.E.Hartle, H.A.Taylor, Jr., Venus ionosphere: Photochemical and thermal diffusion control of ion composition, Science, 205, 109-112, 1979.

Brace,L.H., R.F.Theis, J.P.Krehbiel, A.F.Nagy, T.M.Donahue, M.B.McElroy, A.Pedersen, Electron temperatures and densities in the Venus ionosphere Pioneer Venus Orbiter electron temperature probe results, Science, 203, 763-765, 1979 a.

Brace,L.H., H.A.Taylor,Jr., .A.Cloutier, R.E.Daniell,Jr., A.F.Nagy, In the configuration of the nightside Venus ionohause Geophys. Res. Letters, 6, 345-348, 1979 b.

Brace L.H., R.F.Theis, W.R.Hoegy, J.H.Wolfe, J.D.Mihalov, C.T.Russell, R.C.Elphic, A.F.Nagy, The dynamic behavior of the Venus ionosphere in response to solar wind interactions, J.Geophys. Res., 85, 7663-7678, 1980.

Brace, L.H., R.F.Theis, W.R.Hoegy, Plasma clouds above the ionopause of Venus and their implications, Planet. Space Sci., 30, 29-37, 1982.

Brace, L.H., R.F.Theis, H.G.Mayr, S.A.Curtis, J.G.Luhman, Holes in the nightside ionosphere of Venus, J. Geophys. Res., 87, 199-211, 1982 b.

Chapman, S., The absorption and dissociative or ionizing effect of monochromatic radiation in an atmosphere of a rotating earth. II. Grazing incidence, Proc. Phys. Soc. London, 43, 483-501, 1931.

Cravens, T.E., T.I.Gombosi, J.U.Kozyra, A.F.Nagy, Model calculations of the dayside ionosphere of Venus: Energetics. J.Geophys. Res., 85, 7778-7786.

Cravens, T.E., A.F.Nagy, L.H.Brace, R.H.Chen, W.C.Knudsen, The energetics of the ionosphere of Venus: A preliminary model based on Pioneer Venus observations, Geophys. Res. Letters, 6, 341-344, 1929.

Cravens, T.E., A.J.Kliore, J.U.Kozyra, A.F.Nagy, The ionospheric peak on the Venus dayside, J. Geophys. Res. 86, 11323-11329, 1981.

Cravens, T.E., S.L.Crawford, A.F.Nagy, T.I.Gombosi, A two-dimensional model of the ionosphere of Venus, J. Geophys. Res., 88, in press, 1983.

Cloutier, P.A., R.F.Tascione, R.E.Daniell, Jr., An electrodynamic model of electric carrents and magnetic fields in the dayside ionosphere of Venus, Planet. Space Sci., 29, 635-652, 1981.

Elphic,R.C., C.T.Russell, J.A.Slavin, L.H.Brace, Observations of the dayside ionopause and ionosphere of Venus, J. Geophys. Res., 85, 7679-7696, 1980 a.

Elphic,R.C., C.T.Russell. J.A.Slavin, L.H.Brace, A.F.Nagy, The location of the dayside ionopause of Venus: Pioneer Venus orbita magnitometer observations, Gephys. Res. Letters, 7, 561-564, 1980 b.

Elphic,R.C., C.T.Russell, J.A.Clavin, L.H.Brace, Observations of the dayside ionopause and ionosphere of Venus, J. Geophys. Res., 85, 7679-7696, 1980.

Fjeldbo,G., B.Seidel, D.Scveetnam, T.Howard, The Mariner 10 radio occultation measurements of the ionosphere of Venus, J. Atmos. Sci., 32, 1232-1236, 1975.

Gringauz,K.I., V.V.Bezrukikh, L.S.Musatov, T.K.Breus, Plasma measurements near Venus onboard Venera-4 spacec aft, Kosmich. Issled. 6, 411-419, 1968.

Gringauz K.I., T,K.Breus, Comparison of ionospheric features of planets in the terrestrial group: Mars, Venus and Earth, Kosmich. Issled., 7, 871-890, 1969.

Gringauz,K.I., V.V.Bezrukikh, T.K.Breus, M.I.Verigin, G.I.Volkov, T.Gombosi, A.P.Remizov, The preliminary results of plasma measurements by wide acceptance angle instruments onboard Venera-9,10 satellites, Kosmich. Issled., 14, 839-851, 1976 a.

Gringauz,K.I., V.V.Bezrukikh, T.K.Breus, T.Gombosi, A.P.Remizov, M.I.Verigin, G.I.Volkov, Plasma observations near Venus onboard the Venera-9 and -10 satellites by means of wide-angle plasma detectors, in Physics of Solar planetary environments, ed. by D.J.Williams, AGU Boulder, Colorado, 1976 b, pp. 918-

Gringauz,K.I., M.Verigin, T.Breus, T.Gombosi, Electron fluxes measured on board Venera-9 and -10 in the optical umbra of Venus: main ionization source in Venus' nighttime ionosphere, preprint Pr-303, Space Research Institute, Academy of Sciences of the USSR, Moscow, 1976 c.

Gringauz,K.I., M.I.Verigin,T.K.Breus, T.Gombosi, The fluxes of electrons measured in the Venus' optical umbra onboard Venera-9 and -10: the maih ionization source of the nightside ionosphere of Venus, Doklady Academii Nauk SSSR, 232, 1039-1042, 1977 a.

Gringauz,K.I., M.I.Verigin, T.K.Breus, T.Gombosi, The interaction of the solar wind electrons in the optical umbra of Venus with the planetary atmosphere - the origin of the nighttime ionosphere, preprint D-250, Space Research Institute, Academy of Sciences of the USSR, Moscow, 1977 b.

Gringauz,K.I., M.I.Verigin, T.K.Breus, T.Gombosi, The interaction of electrons in the optical umbra of Venus with the planetary atmosphere - the origin of the nightside ionosphere, J. Geophys. Res. 84, 2123-2127, 1979.

Gringauz,K.I., M.I.Verigin, T,K.Breus, S.V.Ivanova, Low - energetic electrons in the Venus optical umbra detected by the source of the night ionosphere: Comparison with the Pioneer Venus satellite measurements, Kosmich. Issledov., 19, 430-435, 1981.

Gringauz,K.I., M.I.Verigin, T,K.Breus, L.A.Shvachunova, On the prevailing ionization source in the main ionization peak of Venus night-side ionosphere, preprint Pr-730, Space Research institute , Academy of Sciences of the USSR, Moscow, 1982.

Gringauz,K.I., M.I.Verigin, T.K.Breus, L.A.Shvachunova, On the prevailing ionization source in the main ionization peak of the night-side ionosphere of Venus. Kosmich. Issledov., 21, in press, 1983.

Gavrik,A.L., G.S.Ivanov-Kholodny, A.V.Mihalov, N.A.Savich, L.N.Samoznaev, The formation of the daytime Venusian ionosphere: The results of dual-frequency occultation experiments, In Space Research XX, pp. 231-235, Pergamon Oxford, 1980.

Gavrik,A.L., N.A.Savich, L.N.Samoznaev, The analyzes of difussion processes in the daytime ionosphere of Venus, resting on the Venera 9 and 10 radiooccultation data, Proceding of the XIII International Symposium on Space Technology and Science, Tokyo, 1982.

Grebowsky,J.M., S.A.Curtis, Venus nighttime ionosphere holes: The signatures of parallel electric field acceleration region? Geophys. Res. Letters, 8, 1273-1276, 1981.

Herman,J.R., R.E.Hartle, S.J.Bauer, The dayside ionosphere of Venus, Planet. Space Sci., 19, 443-460, 1971.

Howard,H.T., G.L.Tyler, G.Fjeldbo, A.J.Kliore, G.S.Levy, D.L.Brunn, R.Dickinson, R.E.Edelson, W.L.Martin, R.B.Postal, B.Seidel, T.T.Sesplankis, D.L.Shirley, C.T.Stelzried, D.N.Sweetnam, D.N.Zygielbaum, P.B.Esposito, J.D.Anderson, I.I.Spapiro, R.D.Reasenberg, Venus mass, gravity field, atmosphere and ionosphere as measured by Mariner 10 dual-frequency radius system, Science, 183, 1297-1301, 1974.

Hedin,A.E., H.B.Niemann, W.T.Kasprzak, A.Seiff, Global empirical model of the Venus thermosphere, J.Geophys. Res., 88, 73-83, 1983.

Hoegy W.R., H.H.Brace, R.F.Theis, H.G.Mayr, Electron temperature and heat flow in the nightside ionosphere. J. Geophys. Res., 85,7811-7816, 1980.

Intrilligator D.S., M.R.Collard, J.D.Mihelov, R.C.Whitten, J.H.Wolfe, Electron observations and ion flows from the Pioneer Venus Orbiter plasma analyzer experiment, Science, 205, 116-119, 1979.

Ivanov-Kholodny G.S., M.A.Kolosov, N.A.Savich, Yu.N.Aleksandrov, M.B.Vasil'yev, A.S.Vyshlov, V.M.Dubrovin, A.L.Zaitsev, A.V.Michailov, G.M.Petrov, V.A.Samovol, L.N.Samoznaev, I.A.Sidorenko, A.F.Hasyanov, Daytime ionosphere of Venus as studiedwith Venera 9 and 10 dual-frequency radio occultation experiment, Icarus 39, 209-213, 1979.

Izakov, M.N., O.P.Krasitsky, A.V.Pavlov, Model of the ion composition of the Venus day-side ionosphere, Kosmich. Issledov., 19, 733-748, 1981.

Kliore A.J., G.S.Levy, D.L.Cain, G.Fjeldbo, S.I.Rasool, Atmosphere and ionosphere of Venus from the Mariner-5 S-band radio occultation measurement, Science, 158, 1683-1688, 1967.

Kliore A.J., R.Woo, J.W.Armstrong, I,R.Patel, The polar ionosphere of Venus near the therminator from early Pioneer Venus orbiter occultations, Science, 203, 765-768, 1979.

Kliore A.J., I.R.Patel, A.F.Nagy, T.E.Cravens, T.I.Gombosi, Initial observations of the night-time ionosphere of Venus from Pioneer Venus orbiter radio occultations. Science, 205, 99-102, 1979 b.

Kliore A.J., The ionosphere main peak: behavior with solar zenith angle, in An International conference of the Venus envi-roment, Hyatt Rickeys, Palo Alto, California, nov. 1-6, 1981, p. 74.

Kumar S., D.M.Hunten, Venus: An ionospheric model with an exospheric temperature of 350 K, J. Geophys. Res., 79, 2529-2532, 1974.

Kumar S., Venus nightside ionosphere: A model with keV elec-tron impact ionization, Geophys. Res. Letters, 9, 595-598, 1982.

Knudsen W.C., K.Spenner, R.C.Whitten, J.R.Spreiter, K.L.Miller, V.Novak, Thermal structure and major ion composition of the Venus ionosphere: First RPA results from Venus orbiter, Science, 203, 757-763, 1979 a.

Knudsen W.C., K.Spenner, R.C.Whitten, J.R.Spreiter, K.L.Mil-ler, V.Novak, Thermal structure and energy influx to the day and nightside Venus ionosphere, Science, 205, 105-107, 1979 b.

Knudsen W.C., K.Spenner, P.F.Michelson, R.C.Whitten, K.L.Miller, V.Novak, Suprathermal electron energy distribution within the dayside Venus ionosphere, J. Geophys. Res., 85, 7754-7758, 1980 a.

Knudsen W.C., K.Spenner, K.L.Miller, V.Novak. Transport of ionospheric O^+ ions across the Venus terminator and implications, J.Geophys. Res., 85, 7803-7810, 1980 b.

Knudsen W.C., K.Spenner, K.L.Miller, Antisolar acceleration of ionospheric plasma across the Venus terminator, Geophys. Res. Letters, 8, 241-244, 1981.

Luhmann J.G., R.C.Elphic, C.T.Rassell, J.A.Slavin, J.D.Mihalov, Observations of large scale steady magnetic fields in the nightside Venus ionosphere and near vake, Geophys. Res. Letters, 8, 517-520, 1981.

Luhmann J.G., R.C.Elphic, C.T.Rassell, J.D.Mihalov, J.H.Wolfe, Observations of large scale steady magnetic fields in the dayside Venus ionosphere, Geophys. Res. Letters, 7, 917-920, 1980.

Mariner Stanford Group, Venus: Ionosphere and atmosphere as measured by dual frequency occultation on Mariner 5, Science, 158, 1678-1683, 1967.

McElroy M.B., Structure of the Venus and Mars atmospheres, J.Geophys. Res., 74, 29-41, 1969.

McElroy M.B., D.F.Strobel, Models for the nighttime Venus ionosphere, J. Geophys. Res., 74, 1118-1127, 1969,

Butler D.M., J.W.Chamberlain, Venus' nightside ionosphere: Its origin and maintenance, J. Geophys. Res., 81, 4757-4760, 1976.

Mihalov J.D., J.H.Wolf, D.S.Intrilligator, Pioneer Venus plasma observations of the solar wind- Venus interaction, J.Geophys. Res., 85, 7613-7624, 1980.

Colin L. The Pioneer Venus program, J. Geophys. Res., 85, 7575-7598, 1980.

Miller K.L., W.C.Knudsen, K.Spenner, R.C.Whitten, V.Novak, Solar zenith angle dependence of ionospheric ion and electron temperatures and density on Venus, J. Geophys. Res., 85, 7759-7764, 1980.

Nagy A.F., T.M.Donahae, S.C.Liu, S.K.Atreya, P.M.Banks, A model of the Venus ionosphere, Geophys. Res. Letters, 2, 83-86, 1975.

Nagy A.F., T.E.Cravens, R.H.Chen, H.A.Taylor, Jr., L.H.Brace, H.C.Brinton, Comparison of calculated and measured ion densities on the dayside of Venus, Science, 205, 107-109, 1979.

Nagy A.F., T.E.Cravens, S.G.Smith, H.A.Taylor, Jr., H.C.Brinton, Model calculations of the dayside ionosphere of Venus: Ionic composition, J. Geophys. Res., 85, 7795-7801, 1980.

Nagy A.F., T.E.Cravens, T.I.Gombosi, Basic theory and model calculations of the Venus ionosphere, in Venus, ed. by D.M.Hunten, L.Colin, T.M.Donahae, V.I.Moroz, Univ. of Arizona press, Tucson, 1983.

Niemann H.B., R.E.Hartle, A.E.Hedin, W.T.Kasprzak, N.W.Spences, D.M.Hunten, G.R.Carignan, Venus upper atmosphere neutral gas composition: First observations of the diurnal variation, Science, 205, 54-56, 1979.

Nieman H.B., W.T.Kasprzak, A.E.Hedin, D.M.Hunten, N.W.Spencer, Mass spectrometric measurements of the neutral gas composition of the thermosphere and exosphere of Venus. - J. Geophys. Res., 85, 7817-7827, 1980.

Perez-de-Tejada, H., Viscous flow cisculation of the shocked solar wind behind Venus, Science, 207, 981-983, 1980.

Russell C.T., R.C.Elphic, Observations of flux ropes of the Venus ionosphere, Nature, 279, 616-618, 1979.

Russell C.T., J.G.Luhman, R.E .Elphic, L.H.Brace, Magnetic field and plasma waves observations in a plasma cloud at Venus, Geophys. Res. Letters, 9, 45-48, 1982.

Russell C.T., J.G.Luhmann, R.C.Elphic, The properties of the low altitude magnetic belt in the Venus ionosphere, in press 1983.

Scarf F.L., W.W.L.Taylor, I.M.Green, Plasma waves near Venus: Initial observations, Science 203, 748-750, 1979.

Schunk R.W., A.F.Nagy, Ionospheres of the terrestrial planets, Rev. Geophys. Space Phys. 18, 813-852, 1980.

Spenner K., W.C.Knudsen, R.C.Whitten, P.F.Michalson, K.L.Miller, V.Novak, On the maintenance of the Venus nighttime ionosphere: Electron precipitation and plasma transport, J.Geophys. Res., 86, 9170-9178, 1981.

Stewart A.I.F., A search for Venusian auroral ultraviolet emission, paper presented at 24 th COSPAR Meeting, Ottawa, Canada, 1982.

Tailor H.A.,Jr., H.C.Brinton, S.J.Bauer, R.E.Hartle, T.M.Donahue, P.A.Clontier, F.C.Michel, R.E.Daniell, Jr., B.H.Blachwell, Ionosphere of Venus: First observations of the dayside ion composition near dawn and dusk, Science, 203, 752-754, 1979 a.

Taylor H.A.,Jr., H.C.Brinton, S.J.Baner, R.E.Hartle, P.A.Cloutier, R.E.Daniell, T.M.Donahue, Ionosphere of Venus: First observations of day-night variation of the ion composition. Science, 205, 96-99, 1979 b.

Taylor H.A.,Jr., H.C.Brinton, S.J.Bauer, R.E.Hartle, P.A.Cloutier, R.E.Daniell, Global observations of the composition and dynamics of the ionosphere of Venus: Implications for the solar wind interaction, J. Geophys. Res., 85, 7765-7777, 1980.

Taylor H.A., Jr., R.E.Hartle, H.B.Niemann, L.H.Brace, R.E.Daniell,Jr., S.J.Baner, A.J.Kliore, Observed composition of the ionosphere of Venus: Implications for the ionization peak and maintenana of the nightside ionosphere, Icarus, 51, 283-295, 1982.

Theis R.F., L.H.Brace, H.G.Mayr, Empirical models of the electron temperature and density in the Venus ionosphere. J.Geophys. Res., 85, 7787-7794, 1980.

Verigin M.I., K.I.Gringauz, T.Gombosi, T.K.Breus, V.V.Bezrukikh, A.P.Remizov, G.I.Volkov, Plasma near Venus from the Venera-9 and Venera-10 wide angle analyzer data, J. Geophys. Res., 83, 3721-3728, 1978.

Vaisberg O.L., D.S.Intrilligator, V.N.Smirnov, An empirical model of the Venusian outer environment. I. The shape of the dayside solar wind ionosphere interface., J.Geophys. Res., 85, 7642-7650, 1980.

Whitten R.C., The daytime upper ionosphere of Venus, J. Geophys. Res., 75, 3707-3714, 1970.

Whitten R.C., L.Colin, The ionospheres of Mars and Venus, Rev. Geophys. Space Phys., 12, 155-192, 1974.

Whitten R.C., B.Baldwin, W.C.Knudsen, K.L.Miller, K.Spenner, The Venus ionosphere at grazing incidence of solar radiation: Transport of plasma to the night ionosphere, Icarus, 51, 261-270, 1982.

Wolfe J., D.S.Intrilligator, J.Mihalov, H.Collard, D.McKibbin, R.Whitten, A.Barnes, Initial observations of the Pioneer Venus Orbiter solar wind plasma experiment, Science, 203, 750-752, 1979.

Captions

FIGURE 1 Height profiles of the electron number-density in the day ionosphere of Venus obtained from the Venera-9, 10 radiooccultation measurements in the dm- ($\lambda_1 \approx 32$ cm) and cm- ($\lambda_2 = \frac{\lambda_1}{4} = 8$ cm) ranges.

FIGURE 2 Height profiles of the electron number-density in the Venus night ionosphere obtained from the Venera-9, 10 radiooccultation measurements [Aleksandrov et al., 1976b].

The dotted curve - the estimated profile of the electron number-density due to collision ionization by the electron fluxes measured from the same probes [Gringauz et al., 1981].

FIGURE 3 Solar-zenith-angle dependence of the electron number-density in the main, n_{em}, and lower, n_{el}, ionization maxima in the Venus ionosphere.

The shaded zone illustrates the interval of the incertainty in the Pioneer-Venus data. The solid and dotted lines show the zenith-angle dependences of the electron number-density plotted for the theory of Chapman's simple layer.

FIGURE 4 Solar-zenith-angle dependence of the height of the main, h_m, and lower, h_l, maxima of the ionization. The designations are the same as in Figure 3

FIGURE 5 Solar-zenith-angle dependence of the ionopause height. from the data of different experiments

[Elphic et al., 1980].

FIGURE 6 Height dependence of the day side ionopause of Venus on the magnetic pressure at the ionopause and the dynamic pressure of the solar wind measured before the shock front [Brace et al., 1980].

FIGURE 7 Solar-zenith-angle dependence of the ion composition in the Venus ionosphere from the Pioneer-Venus data [Taylor et al., 1980].

FIGURE 8 Ion composition in the day ionosphere of Venus from the Pioneer-Venus data.
The dotted lines show the height distributions of ion components in Izakov et al.'s model [1981].

FIGURE 9 Height distributions of ions in the night ionosphere of Venus from the Pioneer-Venus mass-spectrometric data [Taylor et al., 1980].

FIGURE 10 Height profiles of electron and ion temperatures for different solar zenith angles from the Pioneer-Venus data [Knudsen et al., 1980].

FIGURE 11 Sketch of the non-stationary and small-scale events in the Venus ionosphere [Brace et al., 1983].

FIGURE 12 Sketch of the basic photochemical reactions in the Venus ionosphere [Nagy et al., 1983].

FIGURE 13 Comparison of the ion height profiles in the Venus day ionosphere (solid lines) with the modeling data (dotted lines) [Nagy et al., 1980].

FIGURE 14 Electron fluxes for four selected values of the retarding potential measured in the optical shadow

of Venus by Venera-9, -10.
[Gringauz et al., 1982, 1983]. The thin broken line shows the energy spectrum of electrons measured by Venera-9 on October 28, 1975. For a comparison, the energy spectrum of electrons in the Venus ionosphere is given taken from Spenuer et al.'s paper [1981].

FIGURE 15 Distributions of charged particles in the vicinity of the ionization night maximum in the Venus ionosphere.

Figure 15a gives the distribution of individual ion components from the Pioneer-Venus mass-spectrometric (OIMS) data.

Figure 15b gives: the total number-density of ions of the OIMS data (solid line) for the same passage, n_e determined from the radiooccultation data (crosses), the total number-density of ions plotted from the data of Figure 15a (dotted line).

FIGURE 16 Electron T_e, ion T_i, and neutral T_n temperatures in the day ionosphere of Venus calculated by Cravens et al. [1980]. To compare the data about electron temperatures measured by means of a Langmur probe (OETR ▲) and ion temperatures measured by means of a retarding-potential analyzer (ORPA ■) on board the Pioneer-Venus are given Gravens et al.,[1980].

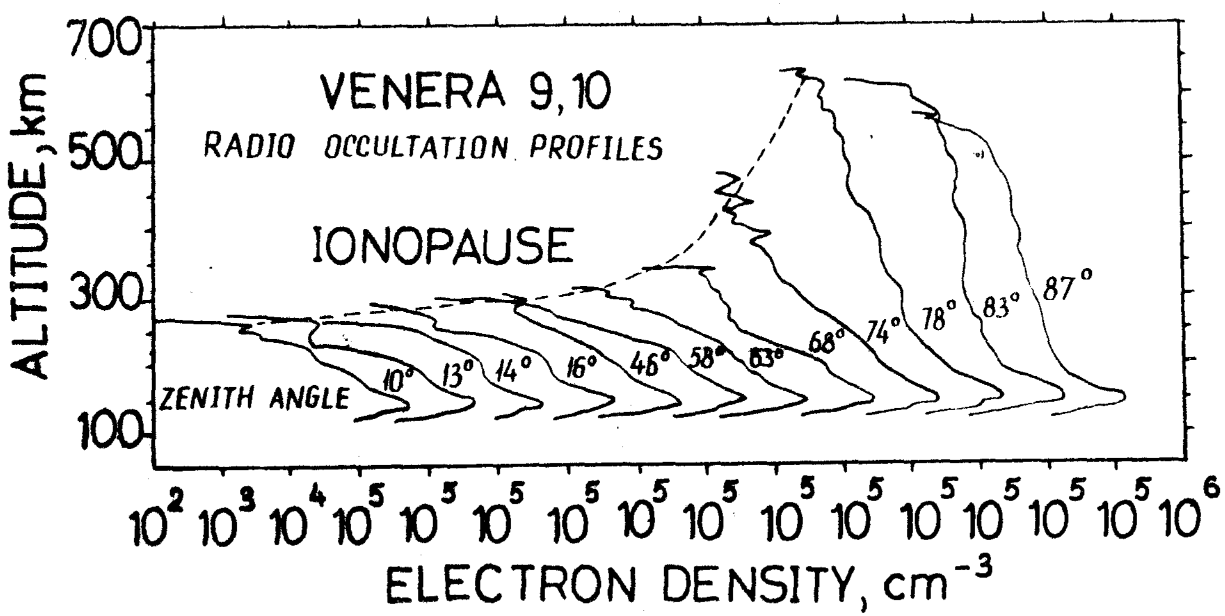
VENERA 9,10
RADIO OCCULTATION PROFILES
IONOPAUSE
ZENITH ANGLE
10° 13° 14° 16° 46° 58° 63° 68° 74° 78° 83° 87°
ALTITUDE, km
700
500
300
100
10^2 10^3 10^4 10^5 10^5 10^5 10^5 10^5 10^5 10^5 10^5 10^5 10^5 10^5 10^5 10^6
ELECTRON DENSITY, cm^-3

Fig. 1

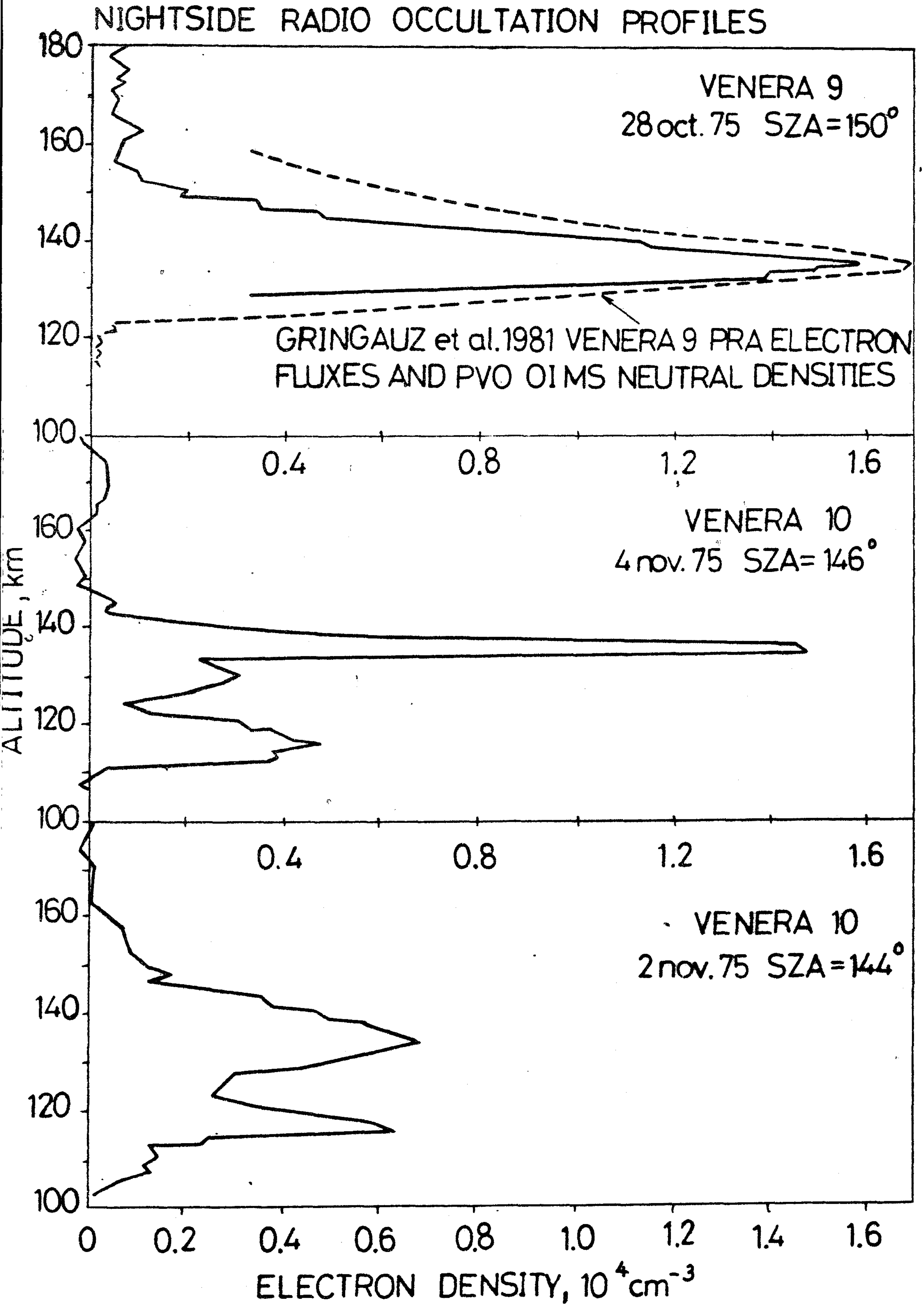
NIGHTSIDE RADIO OCCULTATION PROFILES
180
160
140
120
100
VENERA 9
28 oct. 75 SZA=150°
GRINGAUZ et al. 1981 VENERA 9 PRA ELECTRON FLUXES AND PVO OIMS NEUTRAL DENSITIES
0.4
0.8
1.2
1.6
VENERA 10
4 nov. 75 SZA=146°
ALTITUDE, km
VENERA 10
2 nov. 75 SZA=144°
0
0.2
0.4
0.6
0.8
1.0
1.2
1.4
1.6
ELECTRON DENSITY, $10^4 cm^{-3}$

Fig. 2

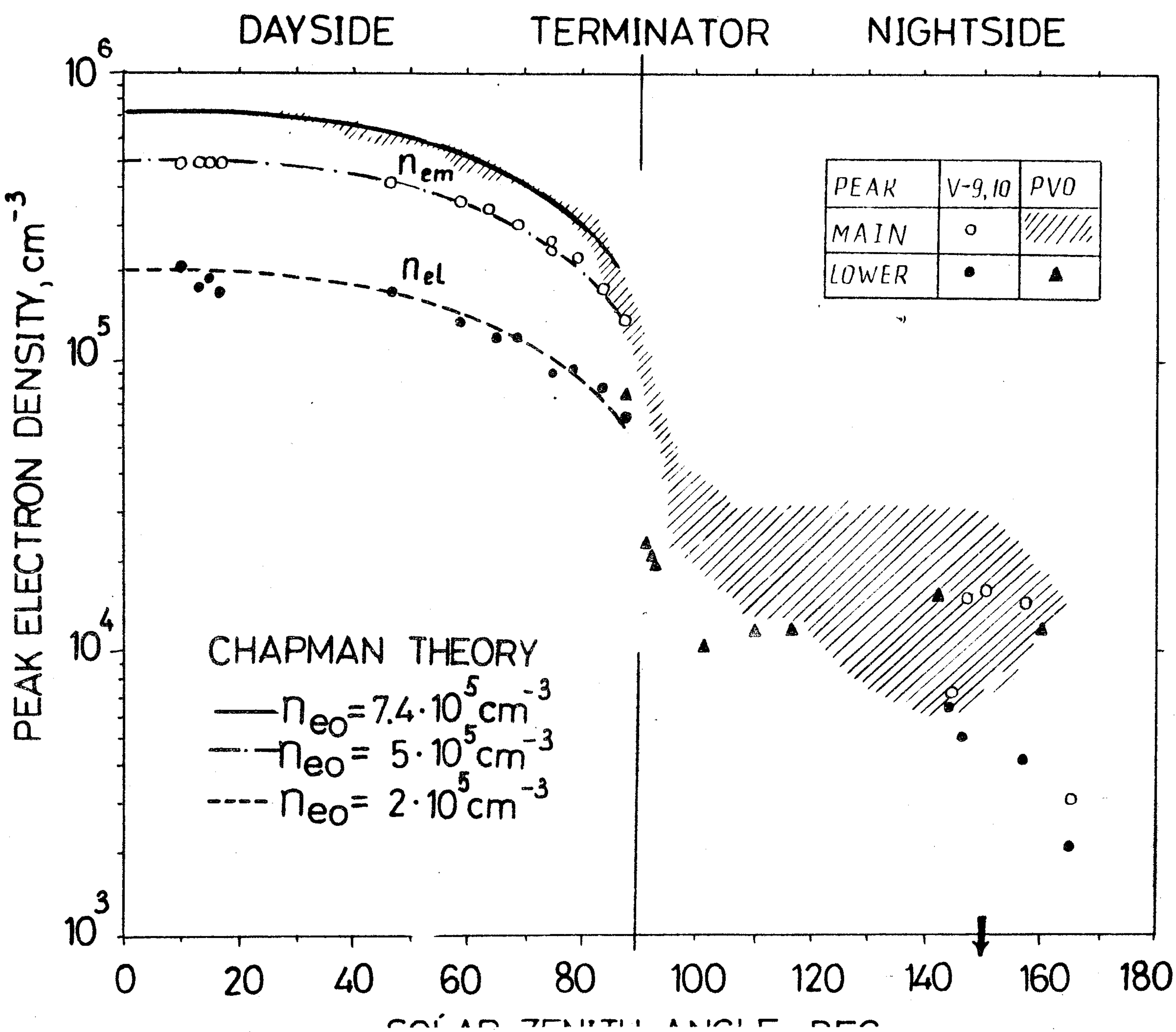
DAYSIDE
TERMINATOR
NIGHTSIDE
PEAK ELECTRON DENSITY, cm^{-3}
10^6
10^5
10^4
10^3
0
20
40
60
80
100
120
140
160
180
n_{em}
n_{el}
PEAK
V-9, 10
PVO
MAIN
LOWER
CHAPMAN THEORY
$n_{eo} = 7.4 \cdot 10^5 cm^{-3}$
$n_{eo} = 5 \cdot 10^5 cm^{-3}$
$n_{eo} = 2 \cdot 10^5 cm^{-3}$

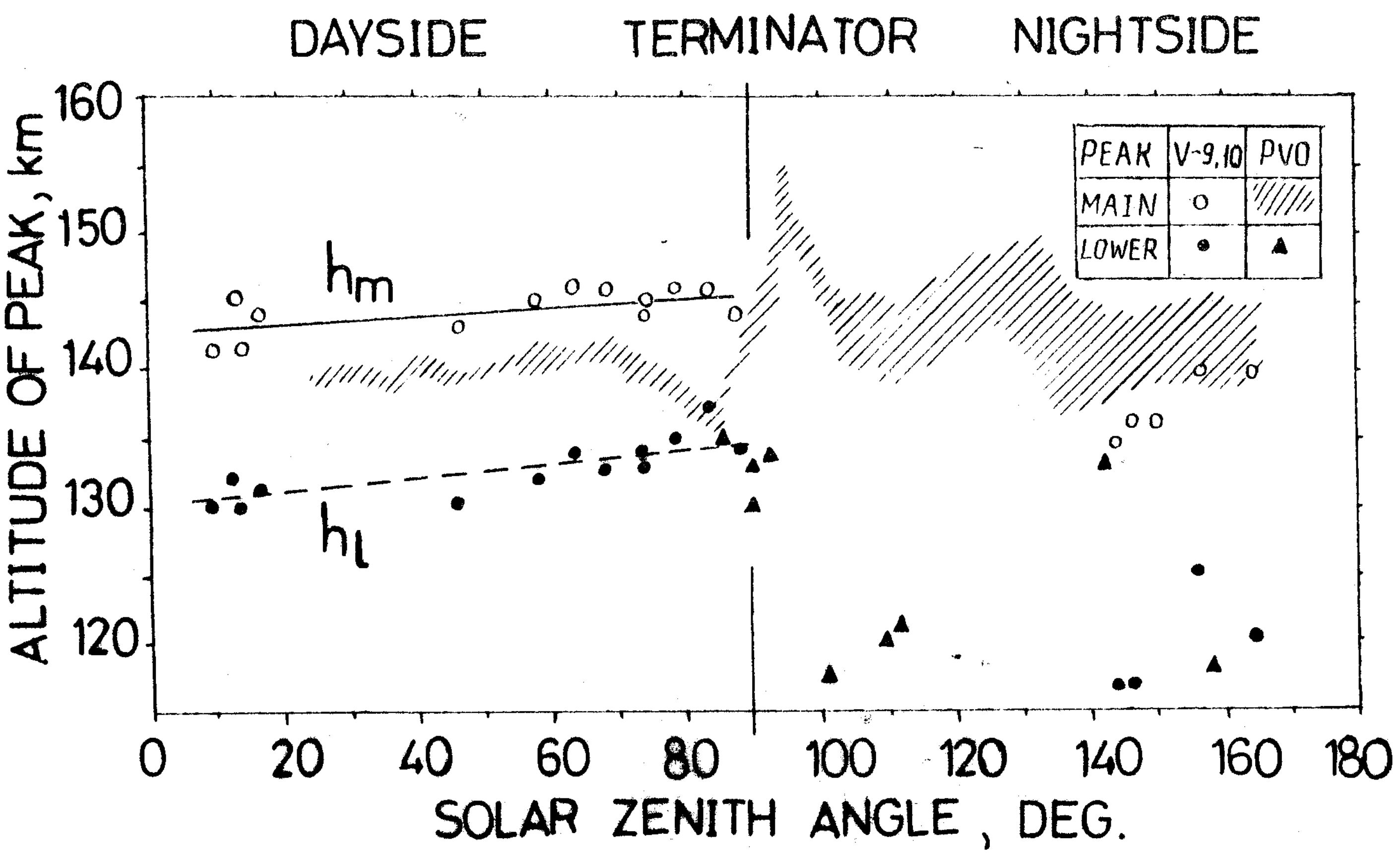
DAYSIDE
TERMINATOR
NIGHTSIDE
ALTITUDE OF PEAK, km
160
150
140
130
120
h_m
h_l
PEAK
V-9,10
PVO
MAIN
LOWER
0
20
40
60
80
100
120
140
160
180
SOLAR ZENITH ANGLE, DEG.

Fig. 4

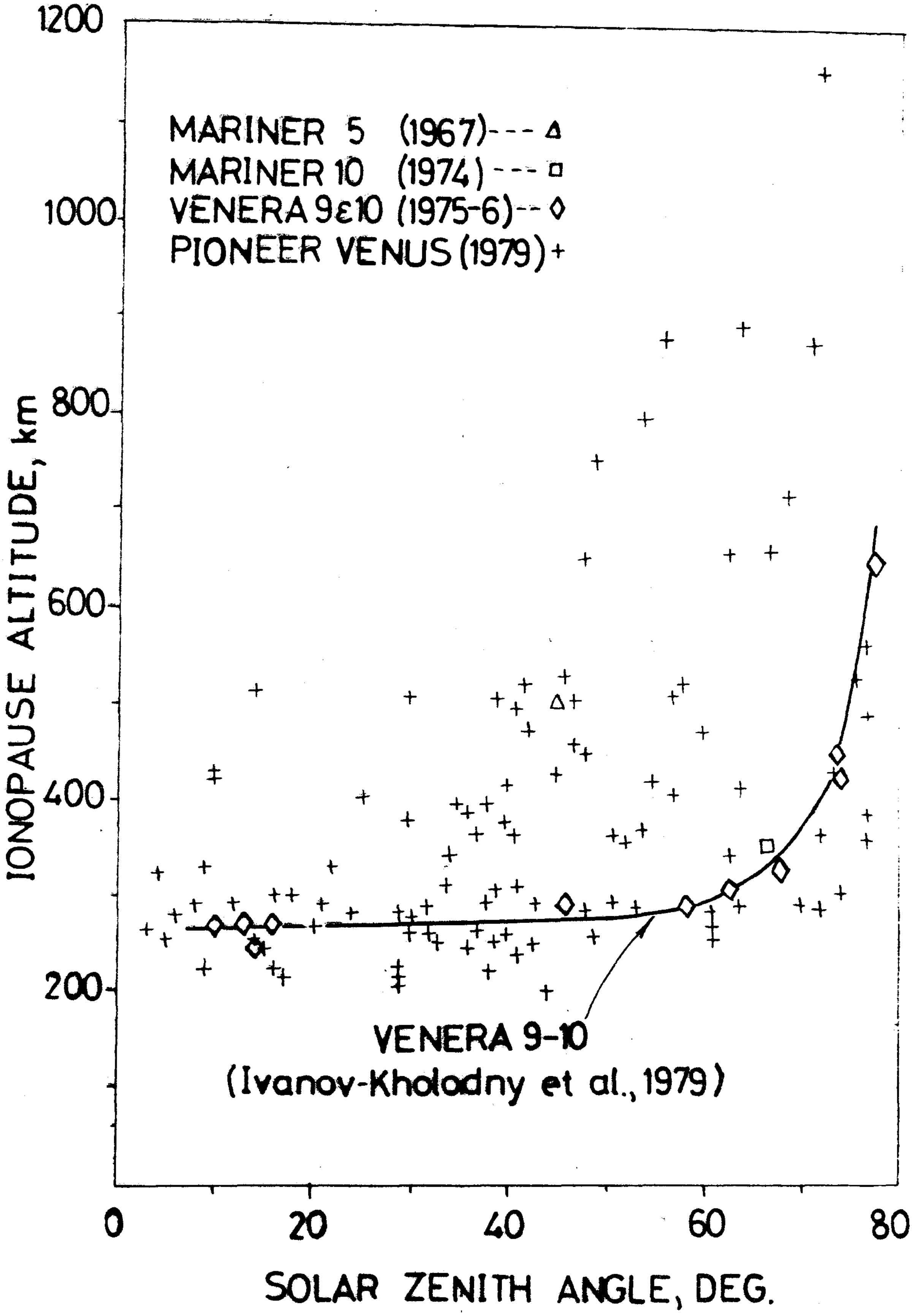
MARINER 5 (1967)--- Δ
MARINER 10 (1974)--- □
VENERA 9&10 (1975-6)-- ◊
PIONEER VENUS (1979) +
VENERA 9-10
(Ivanov-Kholodny et al., 1979)
IONOPAUSE ALTITUDE, km
1200
1000
800
600
400
200
0
20
40
60
80
SOLAR ZENITH ANGLE, DEG.

Fig 5

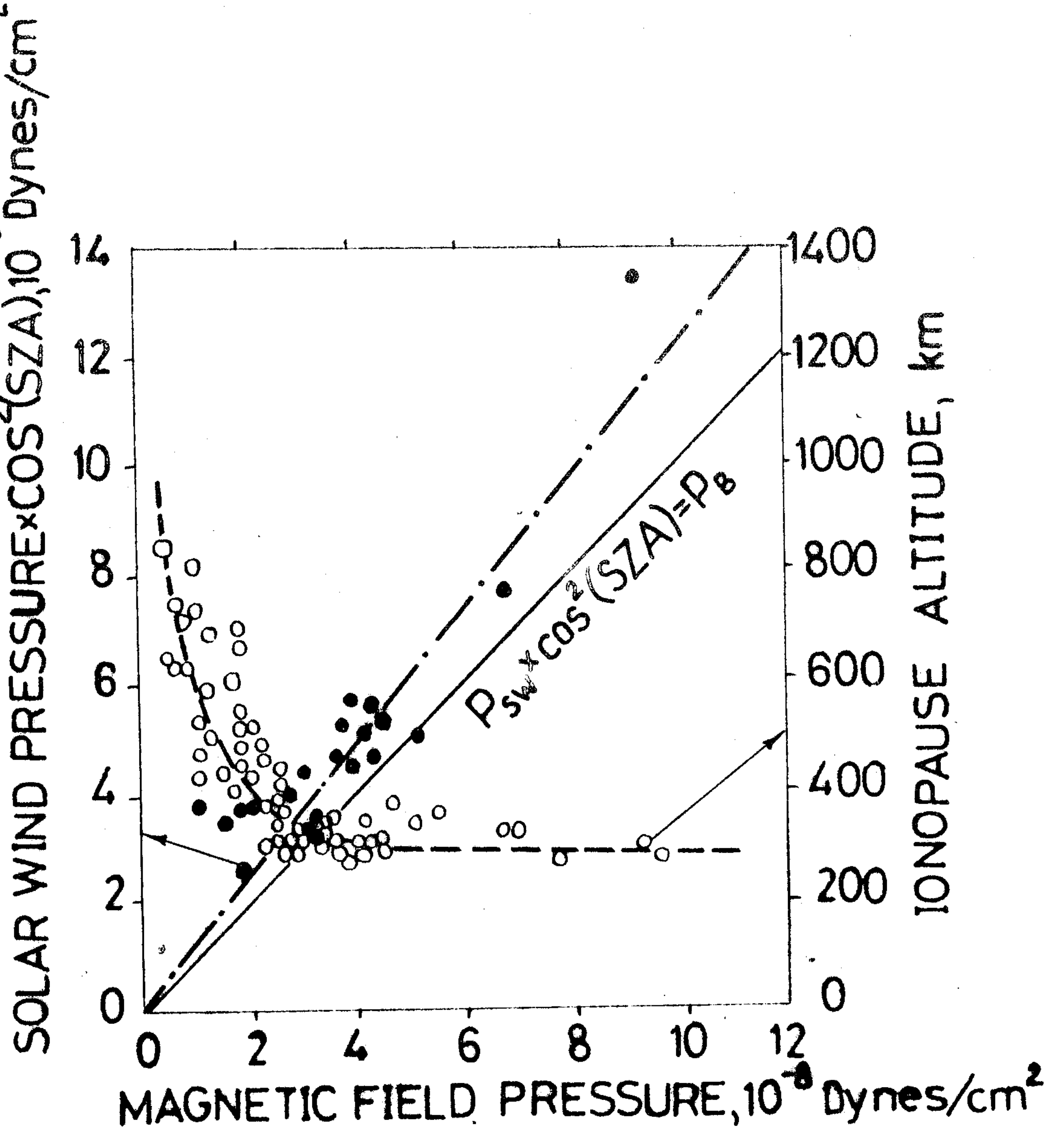
SOLAR WIND PRESSURE×COS²(SZA),10⁻⁸ Dynes/cm²
IONOPAUSE ALTITUDE, km
MAGNETIC FIELD PRESSURE, 10⁻⁸ Dynes/cm²
P_sw × cos²(SZA) = P_B
0
2
4
6
8
10
12
14
0
200
400
600
800
1000
1200
1400

Fig. 6

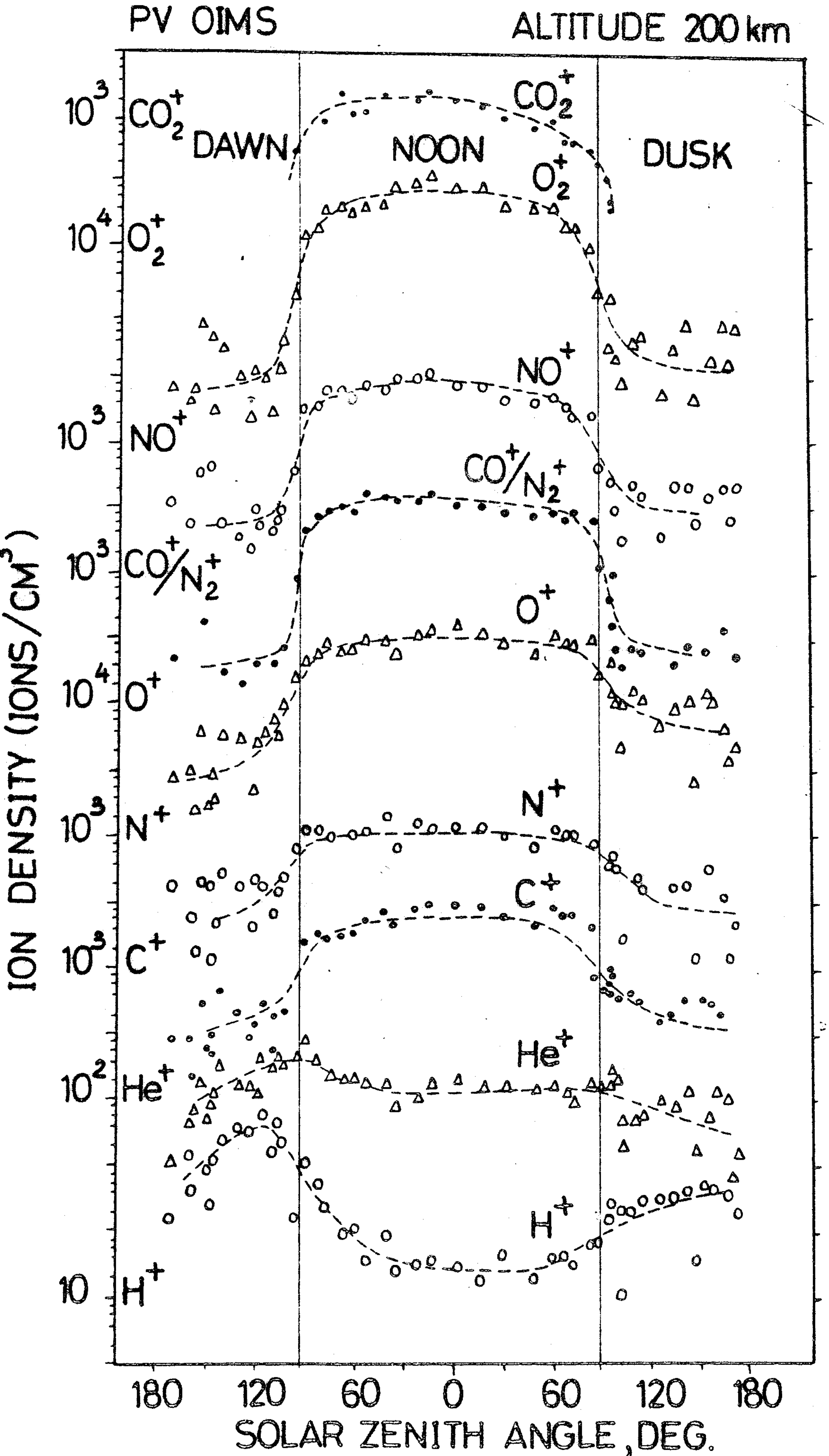
PV OIMS
ALTITUDE 200 km
DAWN
NOON
DUSK
CO_2^+
O_2^+
NO^+
CO^+/N_2^+
O^+
N^+
C^+
He^+
H^+
10^3
10^4
10^3
10^3
10^4
10^3
10^3
10^2
10
ION DENSITY (IONS/CM^3)
180
120
60
0
60
120
180
SOLAR ZENITH ANGLE, DEG.

Fig. 7

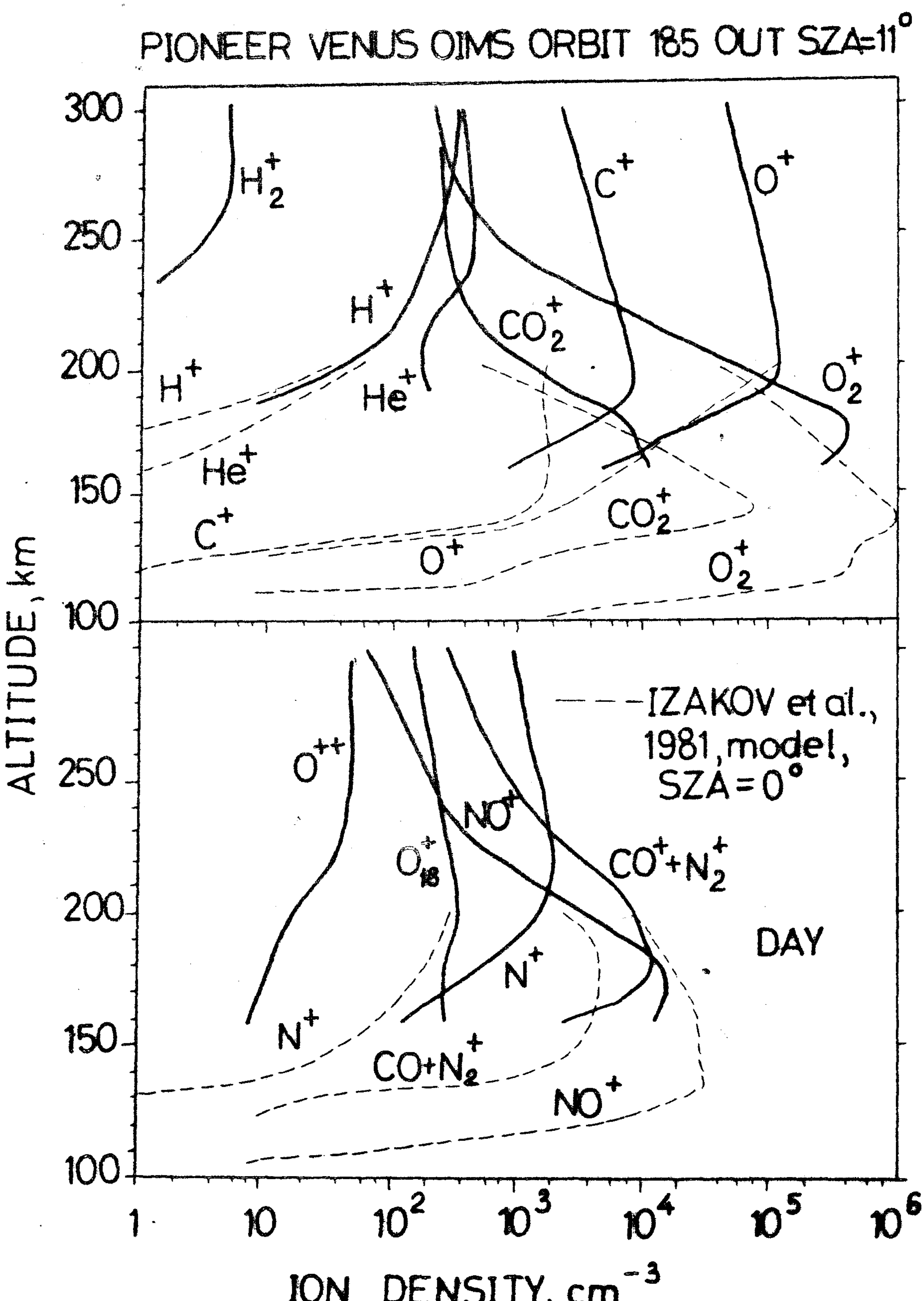

PIONEER VENUS OIMS ORBIT 185 OUT SZA=11°
ALTITUDE, km
ION DENSITY, cm⁻³
H₂⁺
H⁺
He⁺
C⁺
O⁺
CO₂⁺
O₂⁺
O⁺⁺
NO⁺
O₁₈⁺
CO⁺+N₂⁺
N⁺
CO+N₂⁺
IZAKOV et al., 1981, model, SZA = 0°
DAY

Fig. 8

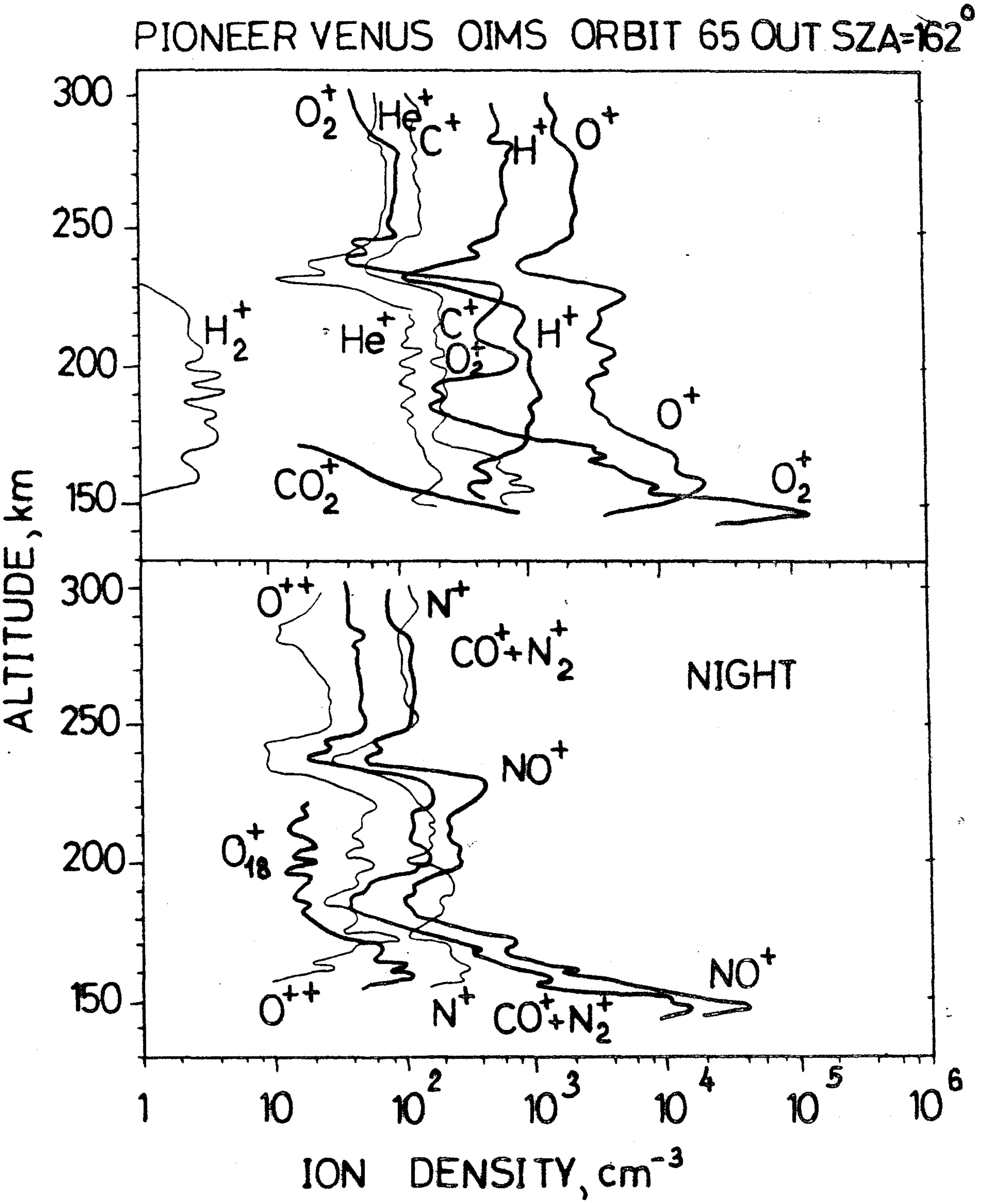
PIONEER VENUS OIMS ORBIT 65 OUT SZA=162°
ALTITUDE, km
300
250
200
150
O_2^+
He^+
C^+
H^+
O^+
H_2^+
CO_2^+
O^{++}
N^+
$CO^+ + N_2^+$
NIGHT
NO^+
O_{18}^+
1
10
10^2
10^3
10^4
10^5
10^6
ION DENSITY, cm^{-3}

Fig. 9

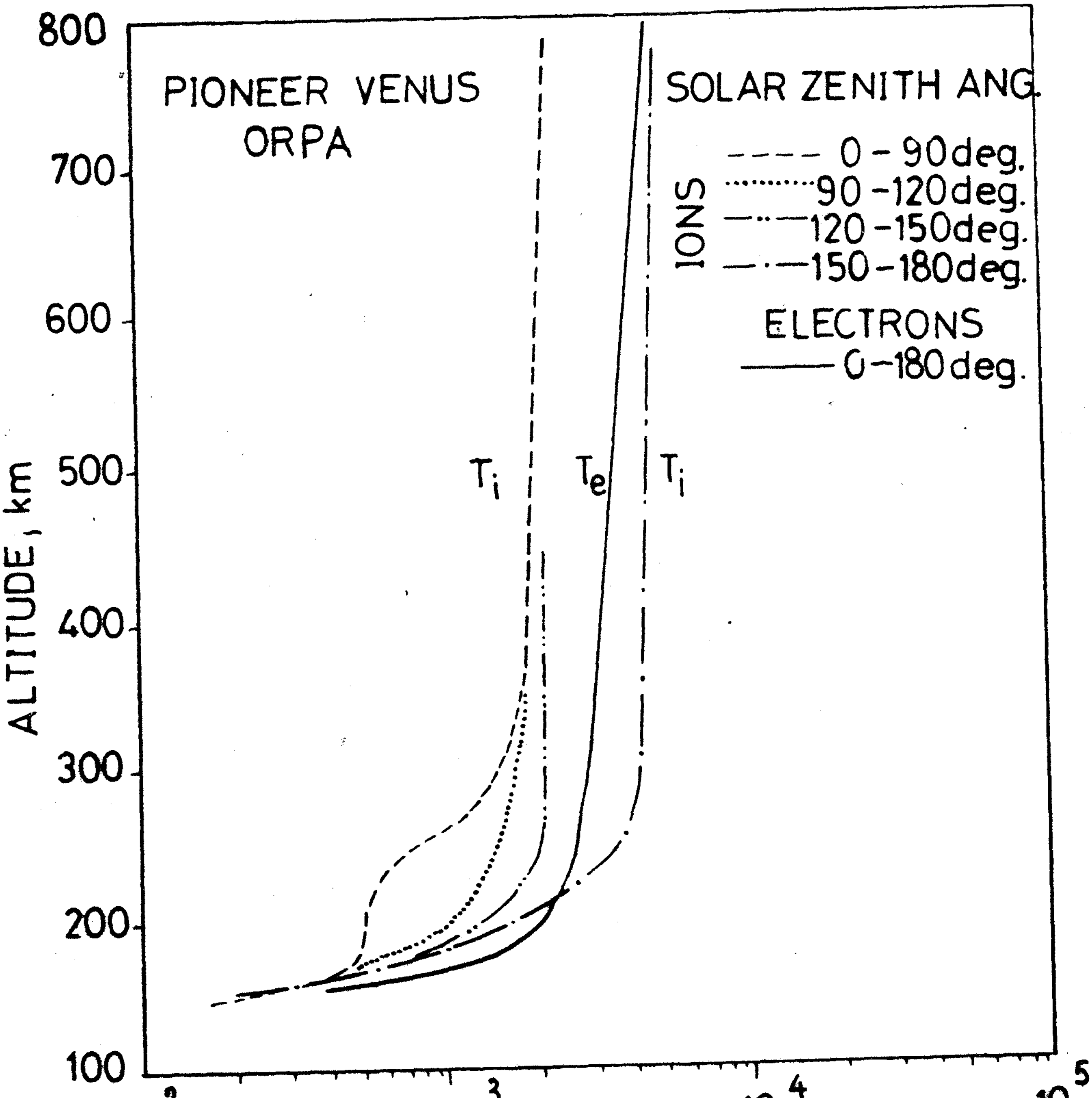
PIONEER VENUS
ORPA
SOLAR ZENITH ANG.
IONS
0 - 90deg.
90 -120deg.
120 -150deg.
150 -180deg.
ELECTRONS
0-180deg.
T_i
T_e
T_i
ALTITUDE, km
800
700
600
500
400
300
200
100
10^2
10^3
10^4
10^5
ION AND ELECTRON TEMPERATURE, °K

Fig. 10

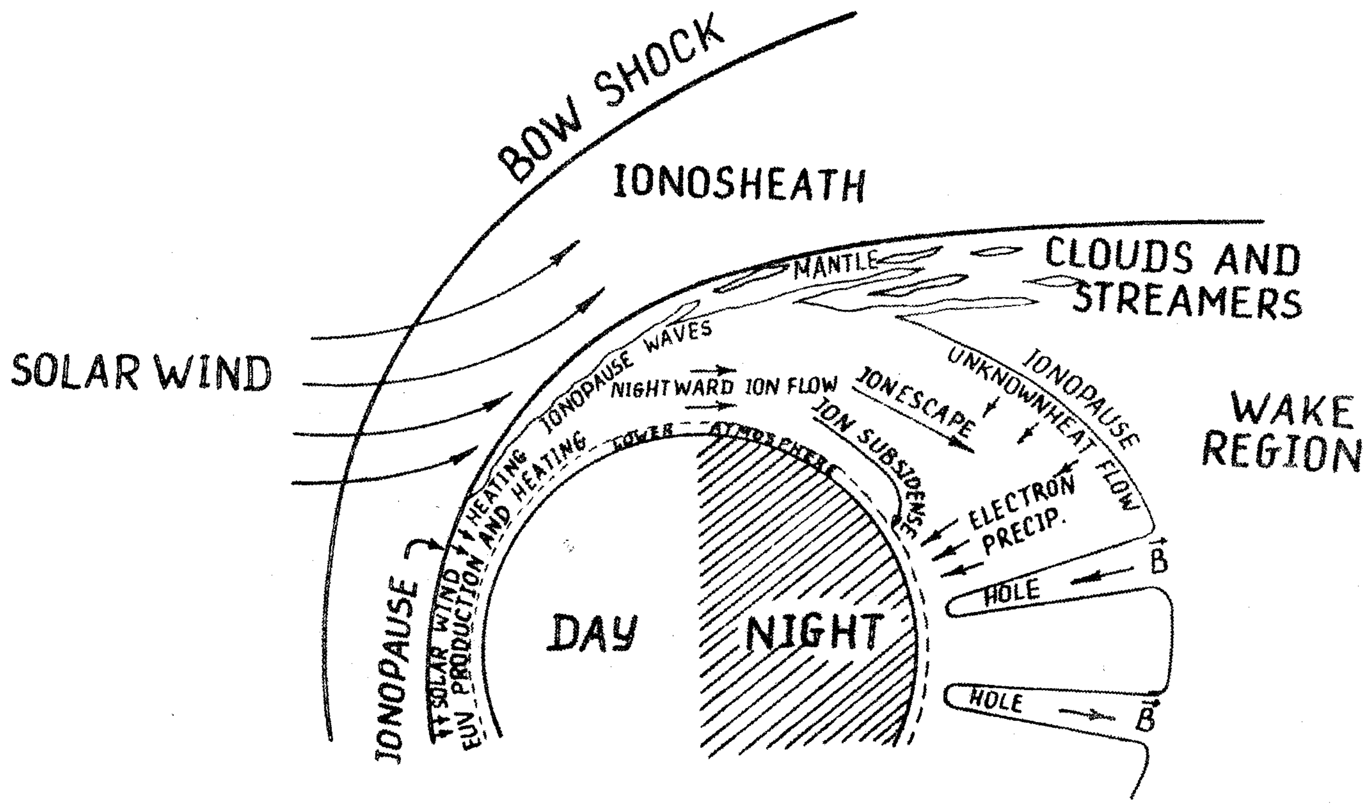
BOW SHOCK
IONOSHEATH
SOLAR WIND
CLOUDS AND STREAMERS
MANTLE
IONOPAUSE WAVES
NIGHTWARD ION FLOW
IONESCAPE
UNKNOWN HEAT FLOW
IONOPAUSE
WAKE REGION
ION SUBSIDENSE
ELECTRON PRECIP.
HEATING
AND HEATING
LOWER ATMOSPHERE
SOLAR WIND
EUV PRODUCTION
IONOPAUSE
DAY
NIGHT
HOLE
HOLE
B
B

Fig. 11

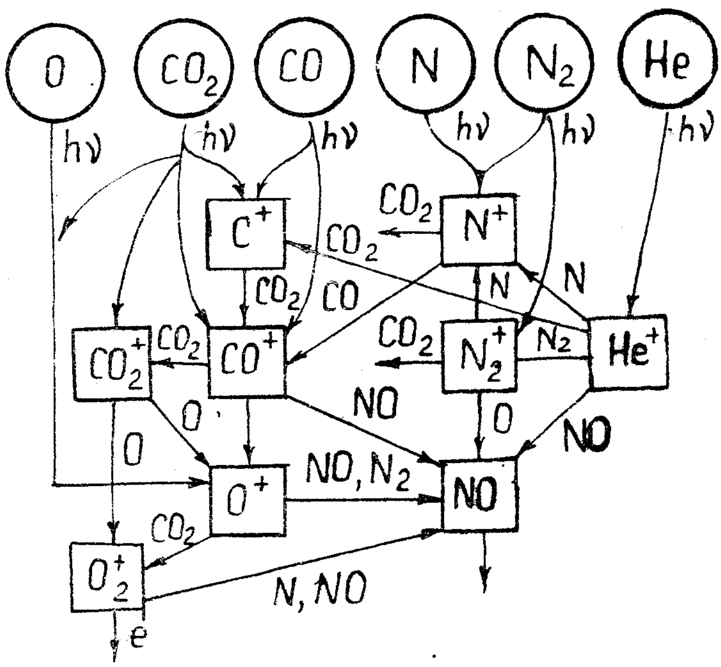

O
CO2
CO
N
N2
He
hν
hν
hν
hν
hν
hν
C+
N+
CO2
CO2
CO2
CO
N
N
CO2+
CO2
CO+
CO2
N2+
N2
He+
O
NO
O
NO
O
O+
NO, N2
NO
CO2
O2+
N, NO
e

Fig. 12

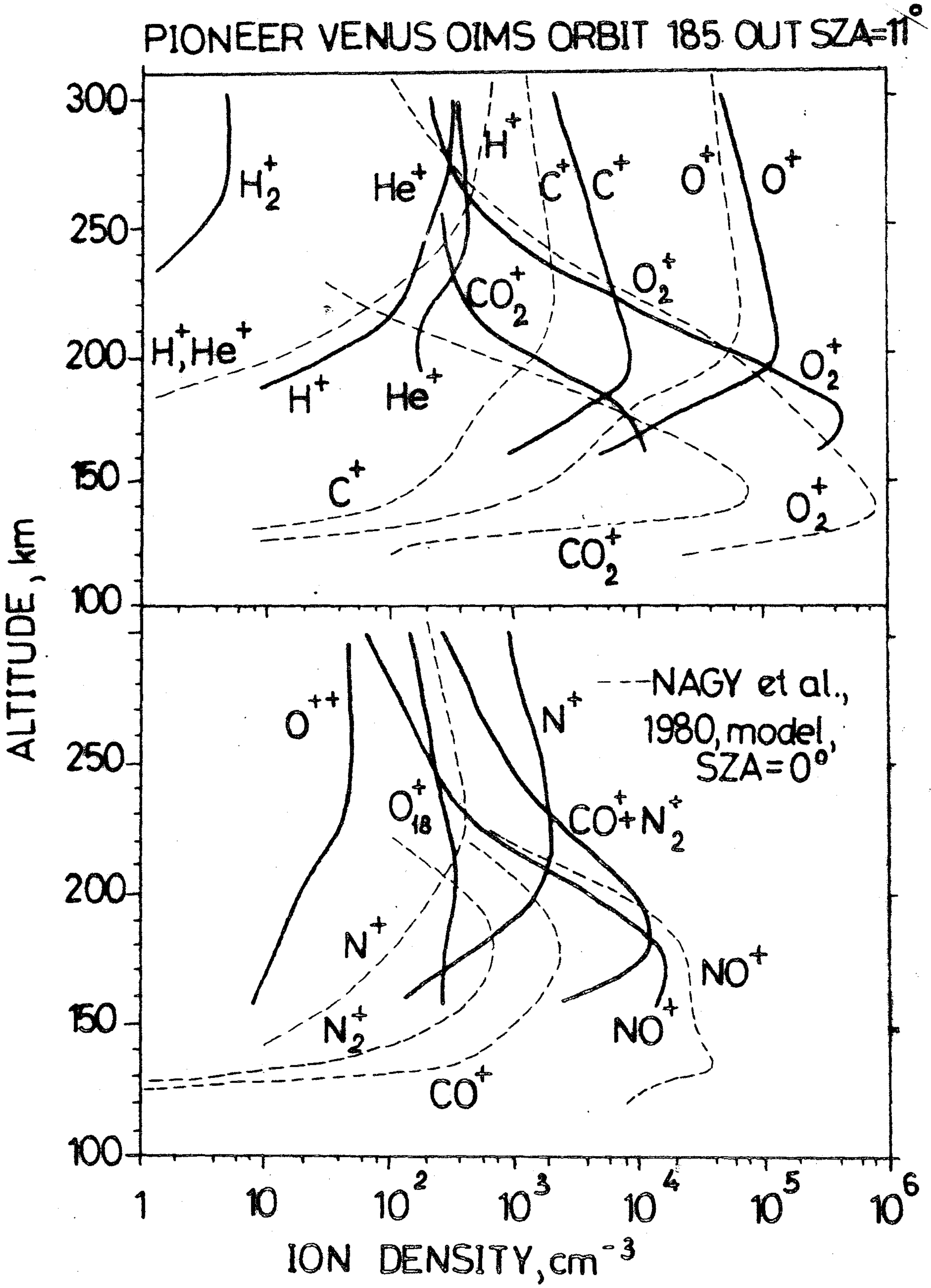
PIONEER VENUS OIMS ORBIT 185 OUT SZA=11°
ALTITUDE, km
ION DENSITY, cm⁻³
H₂⁺
He⁺
H⁺
C⁺
O⁺
O₂⁺
CO₂⁺
H⁺, He⁺
O⁺⁺
N⁺
O₁₈⁺
CO⁺+N₂⁺
N₂⁺
CO⁺
NO⁺
NAGY et al., 1980, model, SZA=0°

Fig. 13

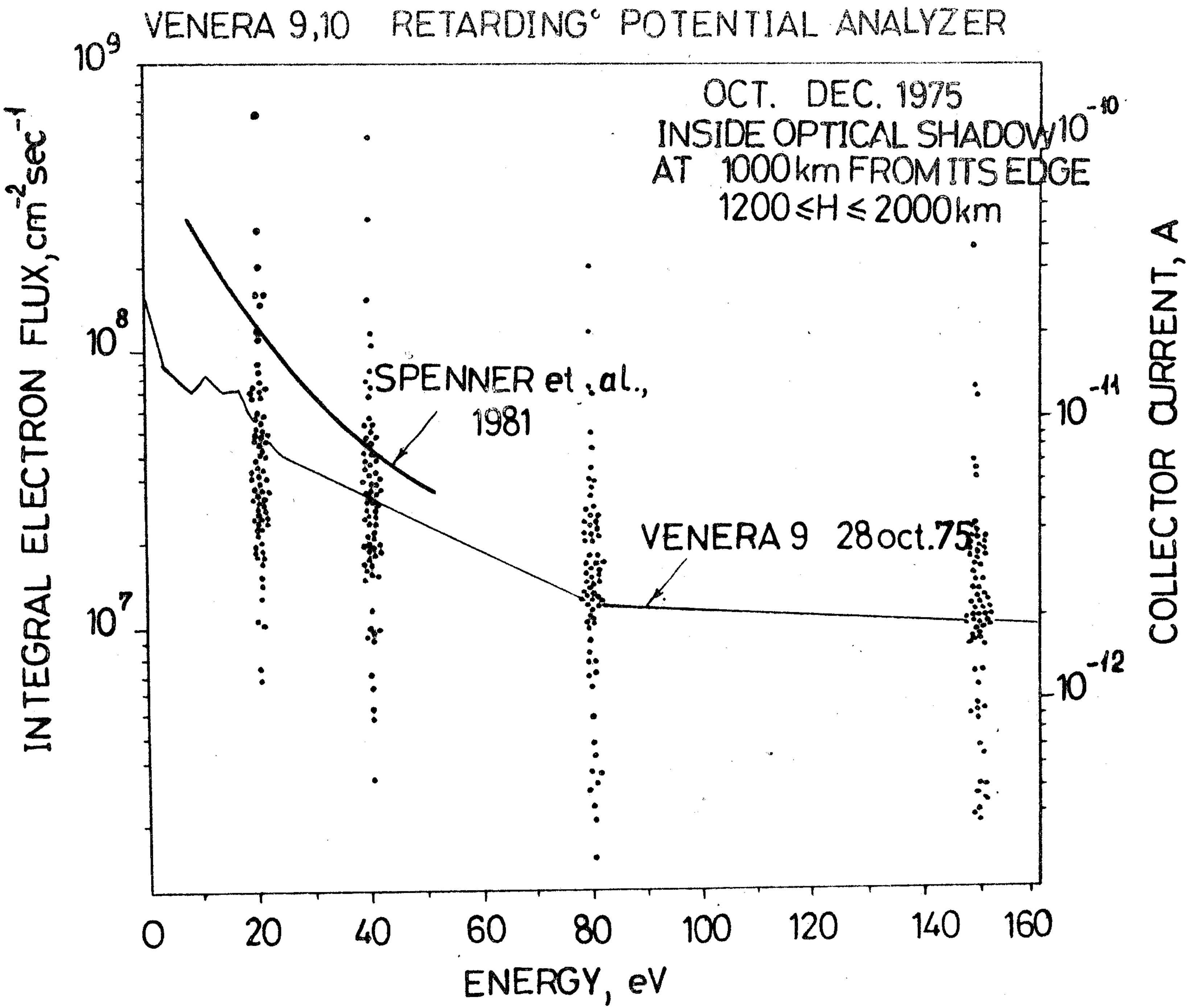
VENERA 9,10 RETARDING POTENTIAL ANALYZER
OCT. DEC. 1975
INSIDE OPTICAL SHADOW
AT 1000km FROM ITS EDGE
1200≤H≤2000km
SPENNER et. al., 1981
VENERA 9 28oct.75
INTEGRAL ELECTRON FLUX, cm^-2 sec^-1
COLLECTOR CURRENT, A
ENERGY, eV
10^9
10^8
10^7
10^-10
10^-11
10^-12
0
20
40
60
80
100
120
140
160

Fig. 14

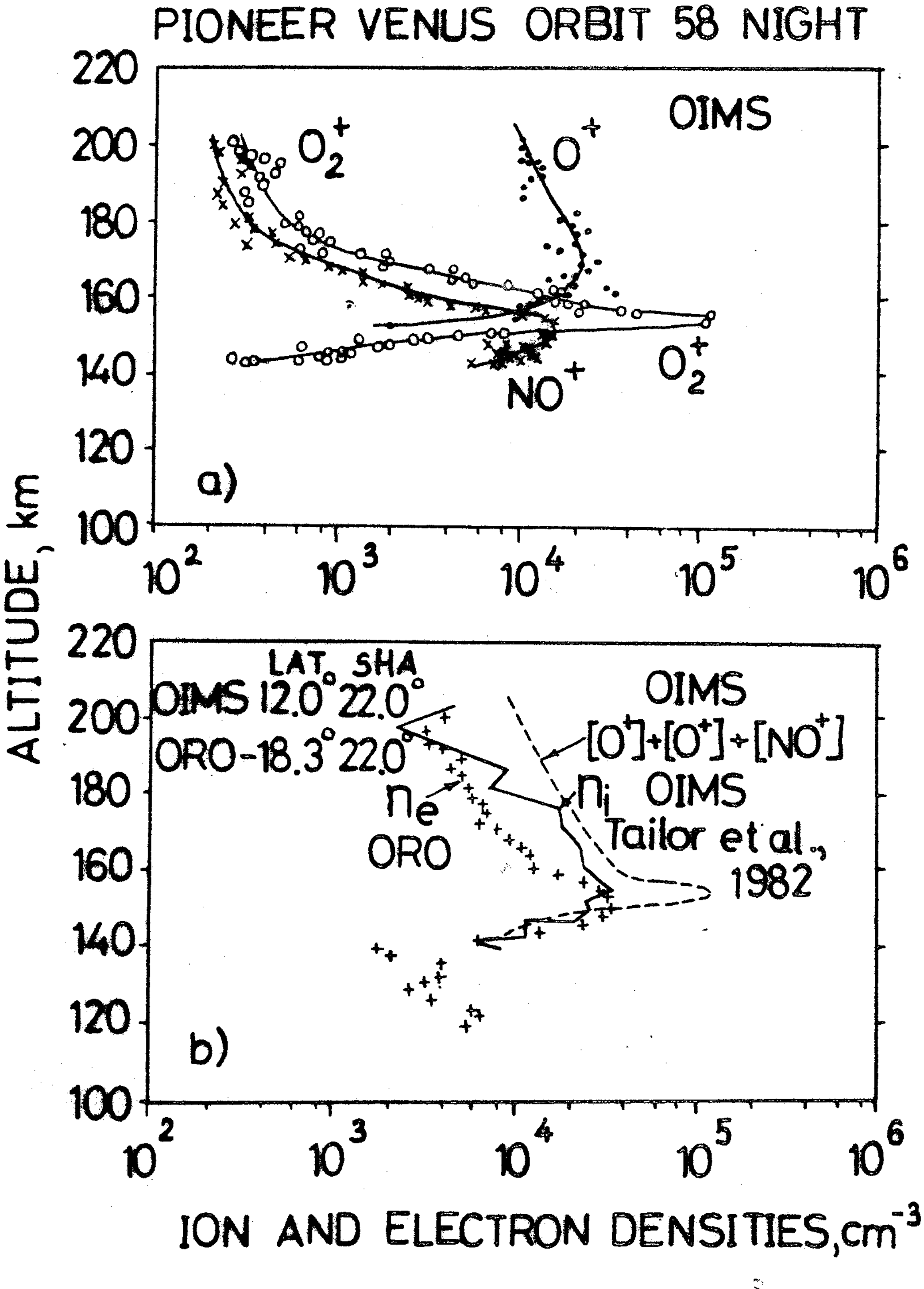
PIONEER VENUS ORBIT 58 NIGHT
OIMS
O_2^+
O^+
O_2^+
NO^+
a)
ALTITUDE, km
LAT. SHA
OIMS 12.0° 22.0°
ORO -18.3° 22.0°
n_e
ORO
OIMS
$[O^+]+[O_2^+]+[NO^+]$
n_i OIMS
Tailor et al., 1982
b)
ION AND ELECTRON DENSITIES, cm^{-3}

Fig. 15

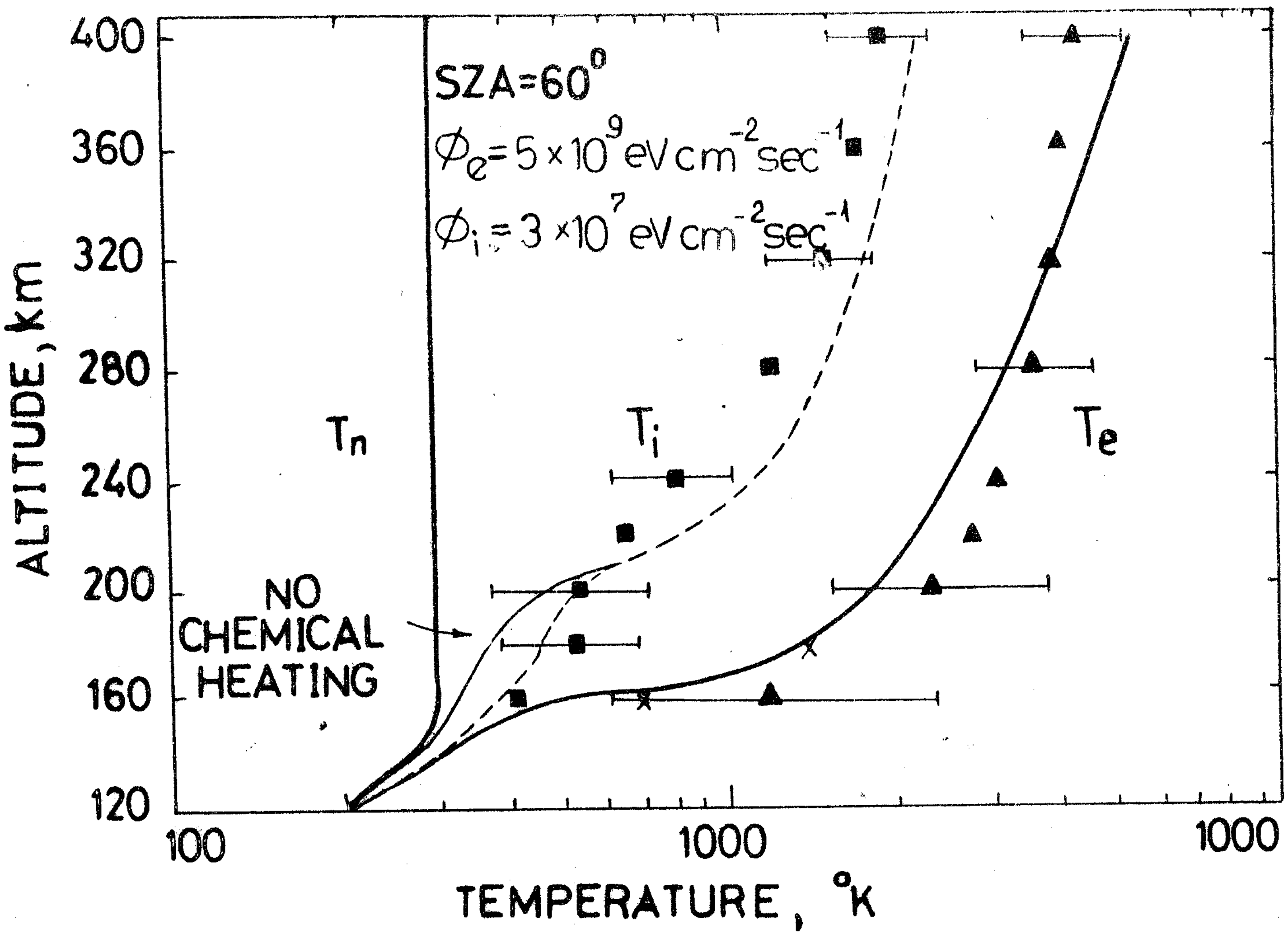
SZA=60°
Φe=5×10⁹ eV cm⁻² sec⁻¹
Φi=3×10⁷ eV cm⁻² sec⁻¹
Tn
Ti
Te
NO CHEMICAL HEATING
ALTITUDE, km
400
360
320
280
240
200
160
120
100
1000
1000
TEMPERATURE, °K

Fig. 16